



1 **Title:**

2 **Climate and demographic impacts on wildfire air pollution hazards**
3 **during the 21st century**

4 **Authors:**

5 Wolfgang Knorr^{*1,2}, Leiwen Jiang^{3,4}, Frank Dentener⁵ & A. Arneth²

6 ¹Physical Geography and Ecosystem Analysis, Lund University, Sölvegatan 12,
7 22362 Lund, Sweden

8 ²KIT/IMK-IFU, Garmisch-Partenkirchen, Germany

9 ³Asian Demographic Research Institute, Shanghai University

10 ⁴National Center for Atmospheric Research, Boulder, Colorado, USA

11 ⁵European Commission, Joint Research Centre, Ispra, Italy.

12 *Corresponding author's email: wolfgang.knorr@nateko.lu.se

13

14 **Abstract:**

15 Wildfires pose a significant risk to human livelihoods and are a substantial health
16 hazard due to emissions of toxic smoke. It is widely believed that climate change,
17 through increasing the frequency of hot weather conditions, will also lead to an
18 increase in wildfire activity. More recently, however, new research has shown that
19 trends in population growth and urbanisation can be as important for fire prediction as
20 changes in climate and atmospheric CO₂, and that under certain scenarios, fire activity
21 may continue to decline through most of the 21st century. The present study re-
22 examines these results from the perspective of air pollution risk, focussing on
23 emissions of airborne particulate matter (PM_{2.5}). We combine an existing ensemble
24 of simulations using a coupled fire-dynamic vegetation model with current
25 observation-based estimates of wildfire emissions to predict future trends. Currently,



26 wildfires PM_{2.5} emissions exceed those from anthropogenic sources in large parts of
27 the world, while emissions from deforestation or peat fires constitute minor sources.
28 We find that for Sub-Saharan Africa and southern China predictions of wildfire
29 pollution risks depend almost entirely on population dynamics, whereas for North
30 Australia and South America, it is mainly determined by climate change, with
31 Southeast Asia lying somewhere in-between. Under a scenario of current legislation
32 of anthropogenic emissions, global high population growth and slow urbanisation,
33 wildfires may cease to be the dominant source in large parts of Sub-Saharan Africa.
34 However, if anthropogenic emissions are strongly reduced, wildfires may both
35 become the dominant source and lie above critical levels for health impacts in large
36 parts of Australia, Africa, Latin America and Russia, and parts of southern China and
37 southern Europe. This implies that controlling anthropogenic emissions will not
38 suffice for attaining the World Health Organization air quality targets.

39 **1 Introduction**

40 Wildfires are a major natural hazard (Bowman et al. 2009) and an important source of
41 air pollutants (Langmann 2009). Of these, emissions of fine aerosol particles, i.e.
42 particulate matter up to a size of 2.5 microns (PM_{2.5}), are of particular health
43 concern, with no known safe levels of PM_{2.5} concentration in air, as noted by the
44 World Health Organization (WHO 2005). While globally, most PM_{2.5} emissions
45 come from human activities, wildfires can be an important source in large, more
46 remote areas (Granier et al. 2011, van der Werf et al. 2010). There is an expectation
47 that such emissions will become more important in the future (Kloster et al. 2010,
48 Knorr et al. 2016a), because of a widely held view among both the general public and
49 members of the research community that wildfire occurrence and severity have been



50 increasing in recent decades, and will continue to increase due to climate change
51 (Doerr and Santin 2016) and efforts to reduce anthropogenic emissions (EEA 2014).
52 Climate warming has already led to frequent hot and dry weather around the
53 globe, increasing the probability of wildfires (Flannigan et al. 2012), and this is
54 expected to continue into the future. Studies based on predicted fire severity indices
55 from climate argue for large increases in burned area as a result of climate warming
56 (Flannigan et al. 2005, Amatulli et al. 2013). However, a long-term increase in the
57 length of the fire season or in weather conditions conducive of wildfires does not
58 necessarily lead to increases in burned area (Doerr and Santin 2016). This is because
59 at longer time scales, vegetation also responds to climate change, as well as directly to
60 rising atmospheric CO₂ levels (Buitenwerf et al. 2012, Donohue et al. 2013). While
61 CO₂ fertilization will lead to increased fuel load, enhancing emissions, it also leads to
62 an increase in woody as opposed to herbaceous vegetation, with lower emissions due
63 to decreased fire spread in shrublands (Kelley et al. 2014, Knorr et al. 2016b). Indeed,
64 simulations with coupled fire-vegetation or statistical climate-envelope models
65 generally show less increase in fire activity until 2100 when accounting not only for
66 climate, but also for these vegetation factors (Krwachuk et al. 2009, Kloster et al.
67 2010, Knorr et al. 2016c).
68 Another factor that has so far received less attention are changes in human
69 population density. Contrary to common perception, higher population density tends
70 to be associated with lower burned area (Archibald et al. 2009, 2010, Lehsten et al.
71 2010, Knorr et al. 2014, Bistinas et al. 2014), even though more humans tend to lead
72 to more, but smaller fires (Archibald et al. 2009, 2010). This can be explained by the
73 concept of the ignition-saturated fire regime, which is reached at very low levels of
74 population density. Above this level, human impact is less manifested as enhancing



75 burned area by providing ignitions, but more by creating barriers to and suppressing
76 fire spread, thus reducing area burned (Guyette et al. 2002). Indeed, coupled
77 vegetation-fire models that include human effects suggest a reduced rate of increase
78 of fire activity during the 21st century compared to simulations not accounting for
79 demographic changes (Kloster et al. 2010), or even a decline in burned area (Knorr et
80 al. 2016c) or emissions (Knorr et al. 2016b) for moderate levels of climate change
81 combined with slow urbanisation and fast population growth. It was found that
82 differences between demographic scenarios can be more important than differences
83 between climate scenarios or climate models. There is also observational evidence for
84 a long-term declining trend in past fire activity or emissions from wildfires (Marlon et
85 al. 2008, Wang et al. 2010, van der Werf et al. 2013), and more recent negative trends
86 in Africa have been related to the expansion of cropland, that is itself a result of
87 increasing population density (Andela and van der Werf 2014).

88 The question is therefore not only how climate and vegetation change in the
89 future will impact on wildfire hazards, but also what the role of total population
90 growth and changes in spatial population distribution is for those predictions.
91 Following a similar study for Europe (Knorr et al. 2016a), we will use PM_{2.5}
92 emissions from wildfires as an example fire hazard to illustrate the relative effects of
93 climate, vegetation and demographics, and base our projections on observation-based
94 wildfire emissions, using vegetation-fire model simulations to project relative
95 changes. The results are meant to be indicative of the importance of demographic and
96 climatic changes for the expected future development of wildfire hazards. All this,
97 however, needs to be seen against a background of considerable uncertainties
98 surrounding future projections of wildfire emissions (Knorr et al. 2016a, Doerr and
99 Santin 2016).



100 **2 Methods**

101 ***2.1 Models and driving data***

102 We use the LPJ-GUESS global dynamic vegetation model (Smith et al. 2001,
103 Ahlström et al. 2012) coupled to the global semi-empirical fire model SIMFIRE
104 (Knorr et al. 2014). A detailed description of the coupling between SIMFIRE and
105 LPJ-GUESS and of methods used to compute wildfire emissions in terms of biomass
106 can be found in Knorr et al. (2016b). LPJ-GUESS is a patch-scale dynamic vegetation
107 model that represents age cohorts and computes vegetation establishment and growth,
108 allocation of carbon pools in living plants, and turnover of carbon in plant litter and
109 soils. SIMFIRE provides burned area to LPJ-GUESS on an annual basis, which then
110 evokes plant mortality according to a plant-functional-type (PFT) dependent
111 probability. Specified fractions of plant litter and live leaf biomass are burnt and
112 emitted into the air in a fire, while the remaining biomass of the killed vegetation is
113 transferred to the litter pool (see Knorr et al. 2012). Population data needed to drive
114 SIMFIRE are based on gridded data from HYDE 3.1 (Klein-Goldewijk et al. 2010) up
115 to 2005, and then re-scaled using per-country relative growth in population and
116 urbanisation rates, retaining the urban masks of the HYDE data. Grid cells with more
117 than 50% past or future cropland area (in either the RCP6.0 or 4.5 land use scenarios
118 of Hurtt et al. 2011) were also excluded (see Knorr et al. 2016b, c for details).

119 In order to compute emissions of chemical species, we use the emission factors of
120 the Global Fire Emissions Database version 4 (GFED 4, Van der Werf et al. 2010,
121 based mainly on Akagi et al. 2011, see <http://www.falw.vu/~gwerf/GFED/GFED4>),
122 which are fixed ratios between emission rates of various pollutant species and rates of
123 combustion of dry biomass differentiated between fires in (1) savannas and
124 grasslands, (2) tropical, (3) boreal and (4) temperate forests. We assign a grid cell to



125 (1) if the dominant PFT (the one with the largest leaf area index at full leaf
126 development) is a grass, to (2) if it is a tropical, to (3) a boreal and to (4) a temperate
127 woody plant (see Knorr et al. 2012 for list of PFTs).

128 ***2.2 Simulations and scenarios***

129 Simulations are driven by output from an ensemble of eight global climate models
130 from the Climate Model Intercomparison Project 5 (CMIP5, Taylor et al. 2012) for
131 two RCP (Representative Concentration Pathway, van Vuuren et al. 2011) climate
132 scenarios: 4.5 (moderate) and 8.5 (high degree of climate change). Simulations for
133 1901 to 2100 are carried out on a global equal-area grid with one by one degree
134 spatial resolution at the equator, but constant east-west spacing of the grid cells when
135 moving towards the poles in order to keep the grid cell area constant (Knorr et al.
136 2016b).

137 Population projections follow the Shared Socioeconomic Pathways (SSPs, Jiang
138 2014). The SSPs are based on qualitative narratives following five different
139 development pathways which have been translated into quantitative projections of a
140 range of socio-economic and biophysical factors. Globally, SSP2 reflects an
141 intermediate case (medium population and economic growth and a central
142 urbanisation case), SSP3 high population growth and slow urbanisation with slow
143 economic development, and SSP5 rapid but fossil-fuel driven economic growth with
144 slow population growth and fast urbanisation. However, there are regional variations
145 in demographic trends under each SSP. In contrast to developing countries and the
146 world as a whole, high-income countries have low population growth for SSP3 but
147 high population growth for SSP5. We did not consider the SSP1 scenario because its
148 sustainability assumptions lead to low emissions and the scenario is therefore not
149 compatible with the RCP8.5 climate scenario, nor did we use SSP4, since it is similar



150 to SSP2 in its population projections. The matrix of three SSPs and two RCP
 151 scenarios represents a wide range of future climate and socio-economic conditions.
 152 In addition to the emission fields simulated by LPJ-GUESS-SIMFIRE, we also use
 153 the GFED4.1s observation-based emissions fields for wildfires (van der Werf et al.
 154 2010, updated using Randerson et al. 2012 and Giglio et al. 2013) aggregated to 0.5
 155 by 0.5 degrees resolution and then re-scaled in time by country or groups of countries
 156 in some cases (following the methodology of Knorr et al. 2016a). For larger countries,
 157 scaling is done by sub-national regions, which were chosen in such a way as to isolate
 158 major fire areas found in GFED4.1s. For a list of regions/countries, see Table A1 in
 159 the Appendix. The use of countries accounts for the high degree of policy or cultural
 160 impact on fire regime (Bowman et al. 2011). In order to account for demographic
 161 effects at the grid-cell scale, we combine a scalar accounting for climate and
 162 vegetation effects, f_{cv} , which is uniform in space across each region, with a scalar
 163 accounting for demographic effects, f_p , which is applied at each grid cell separately:

$$164 \quad E(x, t) = f_{cv}(R(x), t) * f_p(p(x, t)) * E_{GFED}(x) \quad (1)$$

165 with E the re-scaled emissions, x the geographic location on the 0.5 by 0.5 degree grid
 166 used for the analysis, t time, R the region/country found at location x , E_{GFED} the
 167 annual emissions climatology from GFED 4.1s (average for 1997 to 2014). The
 168 population effect, f_p , is equal to the population multiplier of SIMFIRE (Knorr et al.
 169 2016b):

$$170 \quad f_p(p) = \exp(-0.0168 * p'(p)). \quad (2)$$

171 p' here is the minimum of population density p and 100 inhabitants per km², i.e. the
 172 function is constant for values of p above 100 inhabitants per km² (Fig. A1). We have
 173 introduced this cap, which is only used for scaling observation-based inventories by
 174 LPJ-GUESS-SIMFIRE output but not by SIMFIRE itself, in order to prevent large



relative increases in emissions during the scaling procedure, when population density decreases from high values. We thus consider areas with higher population density than 100 per km² to be essentially wildfire free. The combined climate and vegetation effect is defined as

$$f_{cv}(R,t) = \sum_R E(x',t) / [\sum_R E(x',t_0) * \sum_R f_p(p(x',t))]. \quad (3)$$

Here, the sums are over all grid cells x' of the LPJ-GUESS 1-degree equal-area grid that belong to region/country R . For countries where 90% or more of the grid cells of the LPJ-GUESS grid have been excluded because they have a current or future cropland fractions of 50% or higher (highly agricultural regions: Moldavia and Bangladesh), or for which LPJ-GUESS simulates zero current emissions in at least one simulation (Greenland), we set $f_{cv}(R,t) = 1$. Gridded population data is based on HYDE 3.1 (Klein-Goldewijk et al. 2010), and future population patterns are re-scaled from 2005 population data using per-country population increases and changes in urbanization level, retaining the urban masks of the HYDE data (see Knorr et al. 2016c for details).

2.3 Analytical Framework

In our analysis, we focus on four time windows: current, 2030, 2050 and 2090. For current, we use 2010 population fields and annual anthropogenic emission data, as well as the mean annual emissions of GFED4.1s, which span the period 1997-2014. For the future time windows, we again use population fields and anthropogenic emissions from that year, but average emissions simulated by LPJ-GUESS-SIMFIRE spanning a period of 21 years centered on each of these years (i.e. 2020 to 2040 for the 2030 time window, etc.). While LPJ-GUESS-SIMFIRE simulations are carried out on a 1-degree equal-area grid, all spatially explicit analysis is carried out on a global 0.5 by 0.5 degree grid.



200 To assess the relevance of PM_{2.5} emission rates, we both compare them to those
201 from anthropogenic sources, and consider an approximate threshold above which they
202 can be considered relevant for human health and air quality policy. The World Health
203 Organization has adopted an air quality policy target of 10 µg/m³ on an annual
204 average, pointing out that there is no established safe upper limit and that the target
205 was set considering background concentrations of 3–5 µg m⁻³ in North America and
206 Western Europe. We follow here Knorr et al. (2016a) and assume a typical boundary
207 height of 1000 m and a life time of 1/50 years (about 7 days). Pollutants from
208 wildfires are inject into the atmosphere from large plumes, which have a global
209 average height of around 1400 m, but only about 4–5% of wildfire emissions are
210 emitted into the free troposphere, the rest into the boundary layer (Veira et al. 2015).
211 Here, we assume that after about one week, most of PM_{2.5} is either deposited or
212 effectively mixed into the free troposphere. We also neglect horizontal transport
213 between 0.5 by 0.5 degree grid cells and compute an annual budget based on annual
214 mean emissions and pollutant life time. Using these idealized conditions, which are
215 meant as a first guidance, we arrive at a threshold of 0.5 g m⁻² yr⁻¹ for PM_{2.5}
216 emissions corresponding to a mean annual concentration of 10 µg m⁻³. In this
217 analysis, we use 0.2, 0.5 and 1 g m⁻² yr⁻¹ as alternative thresholds spanning a critical
218 range for health and air-quality policy purposes.

219 For anthropogenic emissions, we use the GAINS 4a data (Amann et al., 2011)
220 developed as part of the ECLIPSE project (Granier et al. 2011, Klimont et al. 2013,
221 Stohl et al., 2015) for the years 2010 (for current conditions), 2030 and 2050. There
222 are two future scenarios: current legislation (CLE), and maximum feasible reductions
223 (MFR). MFR corresponds to a policy driven abatement scenario with the aim, among
224 others, to lower PM_{2.5} emissions to a level to minimize health impacts (Amann et al.



225 2011). Following Knorr et al. (2016a), we estimate 2090 CLE emissions assuming
226 constant *per capita* emissions after 2050 but changing population according to the
227 SSP3 scenario. For MFR, 2090 emissions are assumed half of the corresponding 2050
228 levels. As the CLE and MFR scenarios do not account for CO₂ emissions, both are in
229 principal compatible with the CO₂ equivalent greenhouse gas emissions of both RCP
230 scenarios, even though the non-CO₂ greenhouse gas emissions may differ.

231 For a regional analysis, we use a global map of nine major world regions to
232 facilitate a global-scale analysis of our results (see Fig. A2). Of these, three belong to
233 the high-income group of countries of the SSP scenarios (see Jiang and O'Neill 2015):
234 High-income Europe, Australia & New Zealand, and North America. Countries of
235 Europe belonging to the middle-incoming group were assigned Eastern Europe and
236 Central Asia, which also includes Russia. Countries of the Middle East (Israel, oil-
237 rich states of the Persian Gulf) or East Asia (Japan, South Korea) belonging to the
238 high-income group were excluded, which only account for a very small fraction of
239 wildfire emissions in their respective group.

240 **3 Results**

241 ***3.1 Current patterns of wildfire pollutant emissions***

242 The analysis presented in this sub-section concerns exclusively observation-based
243 emission inventories. Currently 14 million km² of land area are affected by wildfire
244 PM_{2.5} emissions that exceed 0.5 g m⁻² yr⁻¹, used as an indicative threshold for serious
245 health impacts, mainly in Sub-Saharan Africa, North America, South Australia,
246 Southeast Asia, and the boreal zone (numbers are for the 0.5 by 0.5 degree grid: 23
247 million km² for a threshold of 0.2 and 8 million km² for a threshold of 1 g m⁻² yr⁻¹)
248 According to the GFED4.1s and ECLIPSE inventories (Fig. 1), PM_{2.5} emissions over
249 large parts of the globe are dominated by wildfires, in particular the boreal zone and



250 the semi-arid tropics. Even in the humid tropics, such as the Amazon basin or
251 Southeast Asia, wildfires are prevalent and deforestation fires still play a
252 comparatively minor role. Only Indonesia is clearly dominated by deforestation and
253 peat fire emissions. Of the nine world regions, four (Sub-Saharan Africa, Latin
254 America & Caribbean, Eastern Europe-Russia-Central Asia and Australia & New
255 Zealand) have higher wildfire than anthropogenic emissions of PM_{2.5} on an annual
256 basis (Table 1).

257 There are large, remote areas where, despite low emission rates, wildfires are the
258 highest emissions source because anthropogenic emissions are even lower. This
259 applies for example to large parts of the boreal zone, central parts of Australia, much
260 of the western US, or the northern part of the Amazon. However, large regions also
261 have emissions above the upper critical range from 0.5 to 1 g m⁻² yr⁻¹, mainly in the
262 boreal-forest areas (Alaska, Canada, Russia), the semi-arid tropics (the African
263 savannas, the areas south of the Amazon basin, Southeast Asia from Myanmar to
264 Cambodia and Northern Australia), and southeastern Australia in the temperate zone.

265 Other pollutants show a similar pattern of dominance (Fig. 2), but with some
266 important differences: for CO and NO_x, anthropogenic sources are more important,
267 and only Sub-Saharan Africa and Australia & New Zealand have emissions of these
268 gases from wildfires close to or surpassing those from anthropogenic sources (Table
269 1). For NO_x, deforestation fires in the Amazon are also of minor importance
270 compared to wildfires (Fig. 2b). For BC, Sub-Saharan Africa has very high but
271 Australia & New Zealand very low anthropogenic sources, which is reflected in the
272 dominance pattern shown in Fig. 2c. BC from wildfires is also important in temperate
273 North America and central Asia.



274 A breakdown of PM_{2.5} emission patterns by population density is shown in Fig.
275 3. It shows current emissions per area averaged over all grid cells of a given region
276 that fall into a certain population-density range. Fig. 3 reveals the expected trend of
277 increasing anthropogenic emissions where more people live. By contrast, for Sub-
278 Saharan Africa, Latin America & Caribbean, Eastern Europe-Russia-Central Asia and
279 South & Southeast Asia, wildfires show peak values with maximum emissions in
280 regions of intermediate population density: Sub-Saharan Africa and Latin America &
281 Caribbean at 1 to 10, Eastern Europe-Russia-Central Asia at 0.1 to 1, and South &
282 Southeast Asia at 10 to 100 people km⁻². Deforestation fires are of minor importance
283 for air pollutant emissions, except for Latin America & Caribbean, where they occur
284 mainly in sparsely populated area, and for South & Southeast Asia, where they are as
285 important as wildfires and most significant in areas of high population density. It is
286 important to note that within South & Southeast Asia (Fig. A2), wildfires occur
287 mainly in South-East Asia proper, but deforestation fires in Indonesia (Fig. 1a).
288 Indonesia is also the only region where emissions from peat fires are relatively
289 important for air pollution. In High-Income Europe and Developing Middle East &
290 North Africa, wildfires show a similar increase with population density as
291 anthropogenic emissions with the consequence that they are much smaller than
292 anthropogenic emissions in all areas (for Developing Middle East & North Africa
293 their magnitude is also very low *per se*). For North America, wildfires have the
294 reverse trend compared to anthropogenic emissions, and for Australia & New Zealand
295 and Developing East Asia, wildfire emissions happen at a similar average rate across
296 all population density categories. These different trends between wildfires and
297 anthropogenic sources lead to a situation where the former become the dominant
298 source below a certain value of population density, which is 10 for Australia & New



299 Zealand, and 1 inhabitant per km² for the other world regions. Developing East Asia
300 also has the highest per-area anthropogenic emissions, which makes wildfire
301 emissions appear to be generally of minor importance compared to current
302 anthropogenic-emission levels.

303 ***3.2 Simulated changes in emissions***

304 In this sub-section we present results from simulation with LPJ-GUESS-SIMFIRE.
305 These differ from those presented in the following sub-sections, where the relative
306 temporal changes from the LPJ-GUESS-SIMFIRE simulations are used to scale
307 current observed emissions (Equ. 1). The ensemble mean PM_{2.5} emission shows a
308 continuous declining trend for Sub-Saharan Africa across both the 20th and the 21st
309 centuries for the moderate climate change scenario (RCP4.5, Fig. 4). Only the two
310 ensembles with fast urbanisation show a slight increasing trend starting after 2050 for
311 the medium population projection (SSP2 with fast urbanisation), or around 2030 for
312 the low population growth scenario (SSP5). The range of predictions across climate
313 models is about as large as the range of predictions across demographic scenarios.
314 The result is surprisingly similar for the high climate change scenario (RCP8.5),
315 where the central SSP2 demographic scenario still shows no clear increase in
316 emissions even towards the end of the 21st century (Fig. 5). For Sub-Saharan Africa,
317 demographic trends are by far the dominant driver of changes in fire regime, while
318 differences between climate scenarios are minor. For the two scenarios with fast
319 urbanisation (with either SSP2 or SSP5 population trends), this region shows a
320 continuing decline in PM_{2.5} emissions from wildfires. The effect of changing only
321 the urbanisation scenario on emissions is approximately half compared to changing
322 both the urbanisation and population scenarios (i.e. changing SSP2 to SSP2 with fast
323 urbanisation vs. changing SSP2 to SSP5; or changing SSP2 to SSP2 with slow



324 urbanisation vs. changing SSP2 to SSP3). This region clearly stands out not only
325 because it has by far the largest share of global wildfire pollutant emissions (Table 1),
326 but also because of its large decline in fire activity driven by population trends.

327 The other two tropical regions, Latin America & Caribbean and South &
328 Southeast Asia, differ from Sub-Saharan Africa in that the simulated historical decline
329 is less steep, and that the future scenarios show an upward trend that is only slight for
330 RCP4.5, but steep for RCP8.5. The range of predictions for only the central SSP2
331 scenario (ensemble ranges for the medium population and central urbanisation
332 scenario, dark grey area in Fig. 4 and 5) is almost as large as that for the entire
333 ensemble, indicating a reduced role for demographic change, with climate change as
334 the main driver. For Latin America & Caribbean, the effect of urbanisation is
335 negligible, whereas urbanisation plays an important role for South & Southeast Asia.
336 However, in the case of moderate climate change (RCP4.5) combined with SSP3 high
337 population growth and slow urbanisation, even in these regions wildfire activity may
338 not increase during the 21st century. The arid Developing Middle East & North Africa
339 region has a similar declining trend, with a reversal around the middle of the 21st
340 century that is strongly dependent of climate scenario.

341 Two northern regions that belong to the middle-income group and therefore have
342 lower population growth with SSP5 than with SSP3 (as have the tropical regions
343 discussed so far) are Eastern Europe-Russia-Central Asia and Developing East Asia.
344 For both, LPJ-GUESS-SIMFIRE simulates no trend during the historical period,
345 except for an increasing upward trend beginning late in the 20th century. The climate
346 scenario has a strong impact on both regions' predictions, and demographics a small,
347 albeit still discernable one. In both regions, urbanisation plays an important role as



348 seen in the difference between SSP2 with central and SSP2 with slow/fast
349 urbanisation.

350 North America and High-Income Europe have a similar temporal profile as
351 Eastern Europe-Russia-Central Asia, but with the order of demographic scenarios
352 reversed. For North America, demographics are predicted to play only a minor role
353 compared to climate change, but for High-Income Europe, there is still a marked
354 influence even though changing the demographic scenario does not change the
355 general trend in predictions. Here, differences between urbanisation scenarios are
356 unimportant, but SSP5, which here has the highest population growth, leads to
357 markedly higher predictions compared to SSP3 with low population growth. Another
358 region that belongs to the high-income group but where most wildfire emissions are
359 from the tropics (Australia & New Zealand, cf. Fig. 1) stands out as showing almost
360 no change in fire activity across both centuries. Only for RCP8.5 there is a very slight
361 increase, and difference between demographic scenarios have almost no impact on the
362 results.

363 We also note that simulations with LPJ-GUESS-SIMFIRE sometimes differ
364 substantially from GFED4.1s (Fig. 4, 5, Table 1), and show in particular higher
365 emissions in the boreal zone (e.g. higher for Eastern Europe-Russia-Central Asia than
366 for Latin America & Caribbean, and also high emissions for North America). We
367 attribute this to differences in the assumed litter load and combustion completeness
368 between GFED (van der Werf et al. 2010) and SIMFIRE (Knorr et al. 2012). These
369 quantities are generally not well constrained, as noted by Knorr et al. (2012). We
370 expect, however, that the relative change in emissions, which we compute by country
371 (Table A1), is much less affected by those differences. In Fig. 6, we show this relative
372 change from current conditions to 2090 by country/region for the two scenarios that



373 lead to the lowest (SSP3 with RCP4.5) or highest (SSP5 with RCP8.5) end-century
374 global emissions.

375 For SSP3/RCP4.5, there is again a very pronounced decline in fire activity in
376 most but not all countries of Africa. South Africa, Namibia and in particular
377 Botswana show a relative increase in emissions of up to 50%. The strongest decline is
378 found in parts of West Africa, in particular Nigeria, where wildfires in this scenario
379 almost completely disappear. By contrast, central Europe, which has a pronounced
380 population decline under SSP3, shows a strong increase, albeit from a low base (Fig.
381 1). An arch of countries spanning from Turkey to Southeast Asia also show either a
382 strong decline or only a small increase in fire activity. Western boreal North America
383 (ALK, CAN-W, Table A1) and eastern boreal Russia (RUS-NW) show moderate to
384 strong increases, which are much higher for SSP5/RCP8.5, driven mainly by climate
385 change given the low population density in these regions. A very large increase with
386 SSP5/RCP8.5 by around 150% is found for eastern and southern China (CHN-E),
387 driven by reduced population size, fast urbanization, and climate change. A
388 pronounced increase is found mainly for the northern part of the Amazon basin
389 (BRA-N). For Australia, we find a decline in the north (AUS-N) for both climate
390 scenarios, but a slight to pronounced increase for the remaining areas (demographics
391 in this region play almost no role).

392 ***3.3 Predicted changes in emissions by population density***

393 The strongest change in the distribution of wildfire emissions against population
394 density (cf. Fig. A3) is found for Sub-Saharan Africa under the SSP3 and RCP4.5
395 scenarios, where the 0.1 to 1 and 1 to 10 people per km² categories see a decline by
396 around a factor of 10 between 2010 and 2090 (Fig. 7). As the area extent of these
397 categories hardly changes (dotted lines) and the decline is absent for SSP5/RCP8.5,



the decrease is mainly because population density within a given category increases, which leads to more fire suppression. (Figs. 1, A2). Woody encroachment, which also leads to a decline in fire activity, would respond strongly to the higher CO₂ levels of RCP8.5 (Buitenwerf et al. 2012, Knorr et al. 2016b, c). Conversely, areas with more than 100 people per km² see an increase in both extent and emissions per area, as more people move into fire-prone area in this slow-urbanisation scenario. For the CLE anthropogenic-emissions scenario, we expect most changes in the relative dominance of wildfire vs. anthropogenic emissions to happen in the 10 to 100 people per km² category.

This pattern of increasing emissions in the most densely populated areas is seen for all middle to lower-income regions (all but Australia & New Zealand, North America and High-Income Europe). Of these, Latin America & Caribbean, Eastern Europe-Russia-Central Asia and Developing Middle East & North Africa show relatively small changes in emissions, while for South & Southeast Asia and Developing East Asia, a decline in emissions in sparsely populated regions is accompanied by a similar decline in anthropogenic emissions, so that no significant changes in the relative importance of the two emission sources are expected for this particular scenario. For High-Income Europe, wildfire emissions are projected to remain well below anthropogenic emissions in all categories, while for Australia & New Zealand, a continuing decrease in emissions in the most densely populated category will make wildfire emissions increasingly relevant in such areas. For North America simulated changes in wildfire are also minor and wildfires will continue to be the dominant source mainly in remote areas.

The situation of relative importance changes drastically if we consider the MFR anthropogenic scenario (Fig. 8). According to this scenario combined with RCP8.5



423 climate and SSP5 demographic change (rapid urbanisation, low population growth in
424 low to middle income countries), wildfires could become the dominant emission
425 source in Sub-Saharan Africa and Australia & New Zealand in all population-density
426 categories as early as 2030, and be at least of comparable magnitude as anthropogenic
427 emissions for Latin America & Caribbean and to a lesser extent South & Southeast
428 Asia and Eastern Europe-Russia-Central Asia. High-Income Europe and Developing
429 Middle East & North Africa, who both have the same increasing relationship between
430 emissions and population density for both sources, wildfires will continue to be minor
431 in all categories despite strong reductions in anthropogenic emissions. For Developing
432 East Asia, there is an approximately fourfold increase predicted for wildfire emissions
433 in the 10 to 100 inhabitants per km² category, with the result that they might become
434 comparable to anthropogenic emissions in areas that comprise a rather large
435 population.

436 ***3.4 Future patterns of pollutant exposure***

437 The previous analysis only compared wildfire and anthropogenic emissions, but in
438 some areas, both might be so low that they do not constitute a relevant health hazard.
439 A further analysis therefore considers if wildfire emissions exceed a threshold of 0.5 g
440 m⁻² yr⁻¹ (Fig. 9; see Fig. A4 and A5 for thresholds of 0.2 and 1 g m⁻² yr⁻¹). Large areas
441 in the boreal zone, South America, Central Asia and Australia where wildfires
442 dominate do not reach this level. However, the analysis also reveals the demographic
443 scenario as the main driver of change for Africa. For SSP3, with high population
444 growth and slow urbanisation, many areas drop below this threshold in the future,
445 independent of climate scenario, but not for SSP5 (low population growth and fast
446 urbanisation). For northern Australia, the result is independent of demographic
447 scenario, while RCP4.5 sees a small contraction of high-emission areas, but RCP8.5 a



448 much larger one with an additional zone with high emissions emerging further south.
449 Changes in the boreal zone and South America are slight but new high-emissions
450 areas appear for RCP8.5 (light and dark blue). Larger new high-emission areas are
451 found in southern China, mainly driven by demographic and to a lesser extent climate
452 change. The same result is found for Portugal, but with the opposite demographic
453 scenario as this is a high-income region where SSP5 has low population growth and
454 leads to the extension of high-emission areas. Other temperate areas in North America
455 and Australia see little change in any of the scenarios.

456 If we consider the number of people living in areas exceeding a certain wildfire-
457 emissions threshold, we find an almost universal increase in both the absolute
458 numbers, and the percentage of global population independent of climate and
459 demographic scenario (Table 2). Currently, between 7.9 and 1.8% of world
460 population is affected, depending on where the threshold is set (3.6% for the 0.5 g m^{-2}
461 yr^{-1} threshold used with Fig. 10). Only for the $1 \text{ g m}^{-2} \text{ yr}^{-1}$ threshold and SSP5/RCP4.5
462 scenario, this percentage will very slightly decrease to 1.7% by 2030, but the absolute
463 number still increase from 126 to 146 Million people affected by dangerously high
464 levels of wildfire air pollution. For all other scenarios and for SSP5/RCP4.5 from
465 2050 there will be an increase both in the absolute and relative numbers of affected
466 population. The demographic scenario is also more important than the degree of
467 climate change. For the $0.5 \text{ g m}^{-2} \text{ yr}^{-1}$ threshold, changing the RCP scenario changes
468 the percentage by between 0.1 for 2030 and 0.4 for 2090, but changing from SSP5
469 (low growth, fast urbanisation) to SSP3 (high growth, slow urbanisation) changes the
470 percentage of affected population by between 0.4 for 2030 and 1.2 for 2090. This
471 difference is even more pronounced for the $0.2 \text{ g m}^{-2} \text{ yr}^{-1}$ threshold, while for the 1 g



472 $\text{m}^{-2} \text{yr}^{-1}$ threshold, both climate and demographic change have about the same
473 importance.

474 Absolute numbers of people affected by the intermediate $0.5 \text{ g m}^{-2} \text{yr}^{-1}$ threshold
475 can reach as high as 973 Million for SSP3 with high population growth and slow
476 urbanisation combined with RCP8.5 climate change, from currently 256 Million, i.e.
477 almost four times the current estimate. Finally, the spatial exceedance patterns are
478 predicted to change very little for $0.2 \text{ g m}^{-2} \text{yr}^{-1}$ (Fig. A4), but are similar between the
479 0.2 and $0.5 \text{ g m}^{-2} \text{yr}^{-1}$ cases (Fig. A5). This stands in contrast to the percentage of
480 affected population (Table 2), and can be explained by a change in the geographic
481 location of areas that are either added or subtracted (cf. China in Fig. A4 vs. Africa in
482 Fig. A5).

483 Using the idealized conditions that have led us to the $0.5 \text{ g m}^{-2} \text{yr}^{-1}$ threshold, i.e.
484 1000 m boundary layer height and $1/50 \text{ yr}$ life time of $\text{PM}_{2.5}$, we can calculate a
485 mean annual concentration value for every grid cell and from there a population-
486 weighted average for each of the nine world regions. For six of those regions, the
487 resulting concentration is below $1 \mu\text{g m}^{-3}$ for all years and scenarios and therefore not
488 considered relevant. For the other three, results are shown in Table 3. For Latin
489 America & Caribbean, we only find a small increase, mainly for RCP8.5. For
490 Australia & New Zealand, the increase is more substantial and much higher for
491 RCP8.5, and the results for both regions are almost the same across all demographic
492 scenarios. Both findings are in accordance with Fig. 10. For Sub-Saharan Africa,
493 however, we find a universal decrease in exposure estimates from currently 7.7 to as
494 low as $5.3 \mu\text{g m}^{-2}$ by 2090 for SSP3 with high population growth, slow urbanisation
495 and RCP8.5. Differences between RCP scenarios amount to about $0.1 \mu\text{g m}^{-2}$, but
496 between demographic scenarios to between 0.3 for RCP4.5 by 2030, and 1.3 for



497 RCP4.5 by 2090. There is also a reversal of the order compared to the population
498 affected by the $0.5 \text{ g m}^{-2} \text{ yr}^{-1}$ threshold, which we assume is dominated by Sub-
499 Saharan Africa (Table 1). Here, the idealized exposure in Sub-Saharan Africa is
500 higher for the fast-urbanisation/low population growth scenario (SSP5) than for those
501 with slow-urbanisation/high population growth (SSP3), but the reverse is true for both
502 relative and absolute population in high-emission areas. For both measure of human
503 risk from PM_{2.5} exposure (Tables 1 and 2), changing only the urbanisation scenarios
504 (with the same SSP2 population scenario) has a markedly smaller impact than
505 changing only the population scenario (and keeping either fast or slow urbanisation).

506 **4 Discussion**

507 An important question is whether past climate change has already led to increases in
508 wildfire activity and related pollutant emissions. The many uncertainties associated
509 with modelling wildfire emissions are discussed in detail by Knorr et al. (2012,
510 2016a). This study simulates an increase from around 1980 to 1990 for Russia and
511 North America, which seems to agree with the observation of a climate-driven
512 increase in fire activity in the western U.S. based on data from 1982 to 2012
513 (Westerling, 2016). However, our simulated relative increase is only very slight for
514 the western U.S. region (Fig. A6), and only reaches about 20% by 2090 for RCP8.5
515 (Fig. 6). Doerr and Santin (2016) argue that this increase may be regional and highly
516 policy dependent. Ironically, there is the possibility that the increase has been driven
517 by increased fire suppression, which has led to fewer but more intense fires and more
518 area burned. While past climate-driven increases in fire activity remain debatable, this
519 study shows a general picture of climate-driven increases that may be overridden by
520 demographic changes only in Sub-Saharan Africa.



521 A particularly large relative increase in wildfire emissions is projected for China
522 and the boreal areas of North America and Russia for the RCP8.5 climate scenario.
523 Southern China is also identified as a new area of high risk from wildfire air pollution.
524 While forest fires in China may have received less attention, they can still be
525 substantial, with 670,000 ha area burnt annually between 1950 and 1999 (Shu et al.
526 2003).

527 The present study broadly re-confirms the results of a previous analysis that was
528 based on burned area as a measure of wildfire risk (Knorr et al. 2016c). Sub-Saharan
529 Africa, currently by far the most fire-prone region, is projected to see a
530 demographically driven decline in fire activity, except for a scenario of low
531 population growth and rapid urbanisation. This decline is in agreement with
532 observations of declining burned area linked to demographic trends for northern part
533 of Sub-Saharan Africa (Andela and van der Werf, 2014). At the same time, wildfire
534 risk to humans will broadly increase for almost all scenarios considered. For
535 developing countries, differences between the high and low population growth
536 scenarios tend to be more important for the projected changes in fire hazard than
537 differences between the two climate scenarios. For the developed world and northern
538 wildfire regions, climate and vegetation change appear to be the main drivers.

539 There are some noteworthy differences between the approaches. Fire risk in
540 Knorr et al. (2016c) is based on the probability of a point in space to be affected by
541 wildfire, while the present study focuses on emissions-related hazards and uses PM_{2.5}
542 emissions as an indicator, taking into account the amount of fuel burnt and its
543 efficiency at producing PM_{2.5}. Both aspects are important for how human societies
544 are impacted by fire but represent different types of hazard, as the former relates
545 mainly to potential loss of property, whereas the latter affects human health. While



546 the burned-area study uses output from LPJ-GUESS-SIMFIRE directly, the present
547 one uses observation-based estimated and re-scales them based on smaller regions
548 according to LPJ-GUESS-SIMFIRE projections. This approach has been used before
549 by Knorr et al. (2016a) and accounts for the importance of policy on wildfire
550 occurrence by scaling emissions mostly by country. The importance of policy is
551 evident for example when comparing observed burned area in Scandinavia to adjacent
552 areas of Russia (Giglio et al. 2013). There is also an underlying assumption in both
553 studies that the impact of population density on area burnt within each country is
554 invariant over time. The present study also confirms the important role of PM_{2.5}
555 emissions for wildfire air pollution risks, as other pollutants tend to have a larger
556 relative contribution from anthropogenic sources (Knorr et al. 2016a).

557 LPJ-GUESS-SIMFIRE only simulates wildfires. The predictions presented in this
558 study therefore leave out the possibility of significant increases in deforestation or
559 peat fire sources. Therefore, peat and deforestation fires have been excluded from the
560 predictive part of the present study. Peat fires can be associated with considerable
561 emissions (Page et al. 2002, Kajii et al. 2002), and forest conversion is often
562 accompanied by burning (van der Werf et al. 2010). The comparative analysis shown
563 here, however, shows that globally both are of minor importance except for Southeast
564 Asia. The south-east Asian deforestation and peat fires occur mainly in Indonesia
565 (Field et al. 2009), where they are the dominant pollution source and occur even in
566 more densely populated areas. In other world regions, including Russia, peat fires are
567 of minor importance.

568 Whether or not future land-use change will lead to an increase or a decrease in
569 deforestation, is unknown. Based on four integrated-assessment model realisations of
570 the four RCPs, Hurtt et al. (2011) projected little increase, and if any, then in future



571 crop and pasture areas. However, in studies that examined land-use change from a
572 broader perspective, a much larger range of crop and pasture changes emerged
573 (Eitelberg et al. 2015, Prestele et al. 2016), which makes the relative change of
574 deforestation and wildfires highly uncertain. In the present analysis, declining wildfire
575 emissions are only predicted for Sub-Saharan Africa, where it appears to be related to
576 conversion of savanna to cropland (Andela and van der Werf 2014). Interestingly,
577 increased fire activity is predicted for southern Africa for both climate scenarios, in
578 accordance with the result of Andela and van der Werf, who found a recent increase
579 for that region driven by declining precipitation. We therefore believe that the results
580 of the present study are broadly representative of possible future changes in wildfire
581 risk, even though one needs to take into account that in certain areas, deforestation
582 may remain the main driver of air pollution for a while.

583 Demographic trends will be an important and often the main factor driving
584 changes in wildfire hazards. One factor is that higher population density in rural areas
585 means lower burned area and emissions, but also more people exposed, and vice
586 versa. In the analysis of burned area patterns by Knorr et al. (2016a), there was a large
587 impact of urbanisation (using the same SSP2 per-country population scenario), with
588 more people living in fire prone areas at slow than at fast urbanisation, but with a
589 relatively minor affect due to overall population change. The average fractional
590 surface area burned in densely populated areas was also higher for slower
591 urbanisation. This is because the suppression of fire by higher population density was
592 over-compensated by a higher number of people living in rural, fire-prone areas. In
593 the present analysis, we find a much smaller impact of urbanisation on the number of
594 people living in areas with high wildfire emissions, but a large impact of total
595 population change. Even though more people tend to suppress fire, the percentage of



596 people living in high-emission areas increases when the overall population is higher.
597 This is the opposite of what we find for the average pollutant concentration levels
598 experienced by the population: For Sub-Saharan Africa, fast urbanisation or high
599 population growth lead to higher emissions in rural areas and overall higher exposure
600 to wildfire pollutants even though people move away from areas with high wildfire
601 activity.

602 While any additional emission source of PM_{2.5} poses a health risk (WHO 2005),
603 in practice wildfires are likely to be ignored by air quality policy if they emit
604 considerably less than anthropogenic sources, in particular as their occurrence tends to
605 be sporadic and of short-term nature. One factor is that wildfire emissions are much
606 more difficult to legislate given the sometimes unexpected results of fire suppression
607 policies (Donovan and Brown 2007). However, we find that in large parts of the
608 world, wildfires are the main air pollutant source. While in many of those regions,
609 wildfires dominate by absence of large anthropogenic sources, Sub-Saharan Africa,
610 Brazil, northern Australia, Southeast Asia and the boreal zone are regions where they
611 not only emit more PM_{2.5} than anthropogenic sources, but emissions are higher than
612 some approximate threshold of health relevance in the region of 0.5 to 1 g m⁻² yr⁻¹.
613 This implies that even controlling all anthropogenic sources, the WHO air quality
614 goals can not be attained.

615 It will therefore of critical importance whether future air quality policy objectives
616 in the various regions will converge to the current WHO guidelines, in which case in
617 these regions fire management will become increasingly important. At current
618 legislation, wildfires will cease to be important for large parts of Africa and
619 considerable parts of South America. If, however, anthropogenic emissions are
620 aggressively curtailed (MFR scenario), wildfires in both regions are predicted to



621 decline less than anthropogenic sources, and climate change will even lead to new
622 areas with wildfire emission levels relevant for air quality policy. Such reductions in
623 anthropogenic emissions would bring those down to levels similar to those of
624 wildfires even in the most densely populated areas, making wildfires the most
625 important pollution source in many regions (Sub-Saharan Africa, Latin America &
626 Caribbean, and to a lesser degree Australia & New Zealand, Eastern Europe-Russia-
627 Central Asia). Because past efforts aimed at a lasting reduction in wildfire activity
628 have largely failed despite high costs (Doerr and Santin 2016), it is questionable
629 whether it is even possible to devise policy measure aimed at bringing down wildfire
630 emissions to meet WHO guidelines. Because wildfires are an essential part of many
631 ecosystems (Bowman et al. 2009), it may therefore better to discount for wildfire
632 emissions as a natural phenomenon and rather adapt urban and suburban planning
633 accordingly (Moritz et al. 2014).

634 This study has some important limitations. It does not consider atmospheric
635 transport or injection height (Gonzi et al. 2015, Sofiev et al. 2012), nor horizontal
636 advection of pollutants, and predictions are based on a single fire and vegetation
637 model. Demographic scenarios do not currently account for changes in the urban
638 mask. It only considers climatological annual emissions during specified time
639 windows, even though wildfires impacts on air quality can have large interannual
640 (Jaffe et al. 2008) and intra-seasonal variations, caused in part by long-range transport
641 (Niemi et al. 2005), which is also not accounted for. It also does not account for
642 relevant secondary emission products, such as ozone from wildfires, which can reach
643 policy relevant levels (Jaffe and Wigder 2012). This contrasts with previous studies
644 on the possible impact of climate change on wildfire-related air pollution hazards
645 have concentrated on changes in meteorological conditions (Jacob and Winner 2008,



Tai et al. 2010) instead of emissions. The study by Kaiser et al. (2012) focuses on current conditions and includes atmospheric transport, using satellite-observed fire radiative energy (Wooster et al. 2005) as well as satellite-derived aerosol optical depth data to constrain wildfire emissions (Kaiser et al. 2012), as opposed to satellite-derived burned area as used by GFED (van der Werf et al. 2010, Giglio et al. 2013). There is also recent progress in the incorporation of injection height (Sofiev et al. 2012) into chemistry-enabled atmospheric general circulation models (Veira et al. 2015).

By contrast, the present study focuses on changes in emissions, and is the first global-scale study to consider changes both climate and demographic drivers of air pollutant emissions from wildfires. Future work should aim at using general circulation models with realistic plume heights for a series of dedicated present and future time slices at combining observed plume height information, fire radiative energy data (for their finer temporal resolution), satellite-derived burned area (for better spatial coverage), projected emission changes from coupled dynamic vegetation-fire models (as the present study), and improved demographic scenarios accounting for changes in urban population density. Such studies would then not only account for long-range transport pollutants and secondary products such as ozone, but also simulate the temporal statistics of pollution events on a daily time scale. Such results could then be used, for example, to assess for how many days the WHO 24-hour PM_{2.5} limit (WHO 2005) is exceeded as a result of wildfire emissions.

5 Summary and conclusions

- So far, there does not seem to be compelling evidence for a long-term trend towards increased pollutant emissions from wildfires due to climate warming. While in the Western U.S. burned area from wildfires seems to have increased



671 and the increase may be linked to climate, the present study simulates only
672 very small relative increase for the region. Most of the predicted increase for
673 North America concerns the boreal forest zone.

674 • Demographic changes appear to be the main driver for the expected changes in
675 wildfire emissions in Sub-Saharan Africa. For a scenario of high population
676 growth and slow urbanisation, there will be large decreases in emissions in
677 many parts of the continent, often dropping below thresholds that make them
678 relevant for air quality policy. The decrease will be much smaller or turn into
679 an increase for a scenario of low population growth and fast urbanisation.

680 • Exposure of humans to PM_{2.5} in Sub-Saharan Africa is expected to drop for
681 all demographic scenarios, but mostly for high population growth and slow
682 urbanisation. Stronger fire suppression by higher rural population outweighs
683 the effect of larger populations in rural areas.

684 • Globally, both the number of people and the percentage of world population
685 exposed to dangerously high PM_{2.5} emissions from wildfires is expected to
686 increase in all scenarios considered. Both relative and absolute increase are
687 highest for high population growth, while the degree of urbanisation plays
688 only a minor role. This is opposite to the average fractional burned area in
689 densely populated regions – a measure of fire risk to properties and lives –
690 where the projected increase was earlier found to depend mostly on the degree
691 of urbanisation.

692 • The goal of reducing PM_{2.5} emissions globally such that the WHO guidelines
693 for PM_{2.5} concentrations are met everywhere may not be attainable because in
694 many regions wildfire emissions will remain above critical thresholds. So far,
695 there is no generally accepted method for wildfire management that has been



696 shown to lead to lasting reductions in fire activity or emissions. The still
697 widely used approach of aggressive fire suppression is not only costly, but
698 may even have led to increased overall fire activity. It may therefore be
699 prudent to accept the existence of wildfires as a natural phenomenon with
700 important ecosystem function and adapt urban planning accordingly.

701 Acknowledgements

702 This work was supported by EU contracts 265148 (Pan-European Gas-Aerosol-
703 climate interaction Study, PEGASOS) and grant 603542 (Land-use change: assessing
704 the net climate forcing, and options for climate change mitigation and adaptation,
705 LUC4C).

706 **Author contributions:** WK conceived of the study, carried out the analysis and wrote
707 the first draft of the manuscript. All authors contributed to discussions and writing.

708 References

- 709 Ahlström, A., Schurgers, G., Arneth, A., and Smith, B.: Robustness and uncertainty in
710 terrestrial ecosystem carbon response to CMIP5 climate change projections, Env.
711 Res. Lett., 7, 044008, doi: 10.1088/1748-9326/7/4/044008, 2012.
- 712 Akagi, S. K., Yokelson, R. J., Wiedinmyer, C., Alvarado, M. J., Reid, J. S., Karl, T.,
713 Crounse, J. D., and Wennberg, P. O.: Emission factors for open and domestic
714 biomass burning for use in atmospheric models, Atmos Chem Phys, 11, 4039-
715 4072, 2011.
- 716 Amann, M., Bertok, I., Borken-Kleefeld, J., Cofala, J., Heyes, C., Höglund-Isaksson,
717 L., Klimont, Z., Nguyen, B., Posch, M., and Rafaj, P.: Cost-effective control of air
718 quality and greenhouse gases in Europe: Modeling and policy applications,
719 Environmental Modelling & Software, 26, 1489-1501, 2011.



- 720 Amatulli, G., Camia, A., and San-Miguel-Ayanz, J.: Estimating future burned areas
 721 under changing climate in the EU-Mediterranean countries, *Sci. Total Environ.*,
 722 450-451, 209-222, 2013.
- 723 Andela, N. and van der Werf, G. R.: Recent trends in African fires driven by cropland
 724 expansion and El Nino to La Nina transition, *Nature Climate Change*, 4, 791-795,
 725 2014.
- 726 Archibald, S., Roy, D. P., van Wilgen, B. W., and Scholes, R. J.: What limits fire? An
 727 examination of drivers of burnt area in Southern Africa, *Global Change Biol*, 15,
 728 613-630, 2009.
- 729 Archibald, S., Scholes, R. J., Roy, D. P., Roberts, G., and Boschetti, L.: Southern
 730 African fire regimes as revealed by remote sensing, *Int J Wildland Fire*, 19, 861-
 731 878, 2010.
- 732 Bistinas, I., Harrison, D. E., Prentice, I. C., and Pereira, J. M. C.: Causal relationships
 733 vs. emergent patterns in the global controls of fire frequency, *Biogeosci.*, 11,
 734 5087–5101, 2014.
- 735 Bowman, D. M. J. S., Balch, J. K., Artaxo, P., Bond, W. J., Carlson, J. M., Cochrane,
 736 M. A., D'Antonio, C. M., DeFries, R. S., Doyle, J. C., Harrison, S. P., Johnston, F.
 737 H., Keeley, J. E., Krawchuk, M. A., Kull, C. A., Marston, J. B., Moritz, M. A.,
 738 Prentice, I. C., Roos, C. I., Scott, A. C., Swetnam, T. W., van der Werf, G. R., and
 739 Pyne, S. J.: Fire in the Earth System, *Science*, 324, 481-484, 2009.
- 740 Buitenwerf, R., Bond, W. J., Stevens, N., and Trollope, W. S. W.: Increased tree
 741 densities in South African savannas: > 50 years of data suggests CO₂ as a driver,
 742 *Global Change Biol*, 18, 675-684, 2012.
- 743 Doerr, S. H. and Santín, C.: Global trends in wildfire and its impacts: perceptions
 744 versus realities in a changing world, *Phil. Trans. R. Soc. B*, 371, 20150345, 2016.



- 745 Donohue, R. J., Roderick, M. L., McVicar, T. R., and Farquhar, G. D.: Impact of CO₂
 746 fertilization on maximum foliage cover across the globe's warm, arid
 747 environments, *Geophys. Res. Lett.*, 40, 3031-3035, 2013.
- 748 Donovan, G. H. and Brown, T. C.: Be careful what you wish for: the legacy of
 749 Smokey Bear, *Frontiers in Ecology and the Environment*, 5, 73-79, 2007.
- 750 EEA: Air quality in Europe - 2014 report, European Environmental Agency Report
 751 No 5/2014, 80 pp., doi:10.2800/22775, 2014.
- 752 Eitelberg, D. A., Vliet, J., and Verburg, P. H.: A review of global potentially available
 753 cropland estimates and their consequences for model-based assessments, *Global*
 754 *Change Biology*, 21, 1236-1248, 2015.
- 755 Field, D. F., van der Werf, G. R., and Shen, S. S. P.: Human amplification of drought-
 756 induced biomass burning in Indonesia since 1960, *Nature Geosci.*, 2, 185-188,
 757 2009.
- 758 Flannigan, M., Logan, K. A., Amiro, B. D., Skinner, W. R., and Stocks, B. J.: Future
 759 area burned in Canada, *Clim. Change*, 72, 1-16, 2005.
- 760 Giglio, L., Randerson, J. T., and van der Werf, G. R.: Analysis of daily, monthly, and
 761 annual burned area using the fourth-generation global fire emissions database
 762 (GFED4), *J Geophys Res-Biogeophys*, 118, 317-328, 2013.
- 763 Gonzi, S., Palmer, P. I., Paugam, R., Wooster, M., and Deeter, M. N.: Quantifying
 764 pyroconvective injection heights using observations of fire energy: sensitivity of
 765 spaceborne observations of carbon monoxide, *Atmos Chem Phys*, 15, 4339-4355,
 766 2015.
- 767 Granier, C., Bessagnet, B., Bond, T., D'Angiola, A., van der Gon, H. D., Frost, G. J.,
 768 Heil, A., Kaiser, J. W., Kinne, S., Klimont, Z., Kloster, S., Lamarque, J. F.,
 769 Liousse, C., Masui, T., Meleux, F., Mieville, A., Ohara, T., Raut, J.-C., Riahi, K.,



- 770 Schultz, M. G., Smith, S. J., Thompson, A., von Aardenne, J., van der Werf, G. R.,
 771 and Vuuren, D. P.: Evolution of anthropogenic and biomass burning emissions of
 772 air pollutants at global and regional scales during the 1980–2010 period, *Clim.*
 773 *Change*, 109, 163–190, 2011.
- 774 Guyette, R. P., Muzika, R. M., and Dey, D. C.: Dynamics of an anthropogenic fire
 775 regime, *Ecosystems*, 5, 472–486, 2002.
- 776 Hurtt, G. C., Chini, L. P., Froking, S., Betts, R. A., Feddema, J., Fischer, G., Fisk, J.
 777 P., Hibbard, K., Houghton, R. A., Janetos, A., Jones, C. D., Kindermann, G.,
 778 Kinoshita, T., Goldewijk, K. K., Riahi, K., Shevliakova, E., Smith, S., Stehfest, E.,
 779 Thomson, A., Thornton, P., van Vuuren, D. P., and Wang, Y. P.: Harmonization of
 780 land-use scenarios for the period 1500–2100: 600 years of global gridded annual
 781 land-use transitions, wood harvest, and resulting secondary lands, *Climatic*
 782 *Change*, 109, 117–161, 2011.
- 783 Jacob, D. J. and Winner, D. A.: Effect of climate change on air quality, *Atmos*
 784 *Environ*, 43, 51–63, 2009.
- 785 Jaffe, D., Chand, D., Hafner, W., Westerling, A., and Spracklen, D.: Influence of fires
 786 on O₃ concentrations in the western US, *Environmental science & technology*, 42,
 787 5885–5891, 2008.
- 788 Jaffe, D. A. and Wigder, N. L.: Ozone production from wildfires: A critical review,
 789 *Atmos. Environ.*, 51, 1–10, 2012.
- 790 Jiang, L.: Internal consistency of demographic assumptions in the shared
 791 socioeconomic pathways, *Popul. Environ.*, 35, 261–285, 2014.
- 792 Jiang, L. and O'Neill, B. C.: Global urbanization projections for the Shared
 793 Socioeconomic Pathways, *Global Environmental Change*, 2015. 2015.
- 794 Kaiser, J. W., Heil, A., Andreae, M. O., Benedetti, A., Chubanova, N., Jones, L.,



- 795 Mocrette, J.-J., Razinger, M., Schultz, M. G., Suttie, M., and van der Werf, G. R.:
796 Biomass burning emissions estimated with a global fire assimilation system based
797 on observed fire radiative power, *Biogeosci.*, 9, 527-554, 2012.
- 798 Kajii, Y., Kato, S., Streets, D. G., Tsai, N. Y., Shvidenko, A., Nilsson, S., McCallum,
799 I., Minko, N. P., Abushenko, N., and Altyntsev, D.: Boreal forest fires in Siberia in
800 1998: Estimation of area burned and emissions of pollutants by advanced very high
801 resolution radiometer satellite data, *Journal of Geophysical Research:*
802 *Atmospheres*, 107, 2002.
- 803 Kelley, D. I. and Harrison, S. P.: Enhanced Australian carbon sink despite increased
804 wildfire during the 21st century, *Environ. Res. Lett.*, 9, 104015, doi: 10.1088/1748-
805 9326/9/10/104015, 2014.
- 806 Klimont, Z., Smith, S. J., and Cofala, J.: The last decade of global anthropogenic
807 sulfur dioxide: 2000-2011 emissions, *Environ. Res. Lett.*, 8, 014003, 2013.
- 808 Kloster, S., Mahowald, N. M., Randerson, J. T., Thornton, P. E., Hoffman, F. M.,
809 Levis, S., Lawrence, P. J., Feddes, J. J., Oleson, K. W., and Lawrence, D. M.:
810 Fire dynamics during the 20th century simulated by the Community Land Model,
811 *Biogeosci.*, 7, 1877-1902, 2010.
- 812 Klein Goldewijk, K., Beusen, A., and Janssen, P.: Long-term dynamic modeling of
813 global population and built-up area in a spatially explicit way: HYDE 3.1,
814 *Holocene*, 20, 565-573, 2010.
- 815 Knorr, W., Lehsten, V., and Arneth, A.: Determinants and predictability of global
816 wildfire emissions, *Atm. Chem. Phys.*, 12, 6845-6861, 2012.
- 817 Knorr, W., Kaminski, T., Arneth, A., and Weber, U.: Impact of human population
818 density on fire frequency at the global scale, *Biogeosci.*, 11, 1085-1102, 2014.
- 819 Knorr, W., Dentener, F., Hantson, S., Jiang, L., Klimont, Z., and Arneth, A.: Air



- 820 quality impacts of European wildfire emissions in a changing climate, Atmos.
 821 Chem. Phys, 16, 5685-5703, 2016a.
- 822 Knorr, W., Jiang, L., and Arneth, A.: Climate, CO₂, and demographic impacts on
 823 global wildfire emissions, Biogeosci., 13, 267-282, 2016b.
- 824 Knorr, W., Arneth, A., and Jiang, L.: Demographic controls of future global fire risk,
 825 Nature Climate Change, doi: 10.1038/NCLIMATE2999, 2016c.
- 826 Krawchuk, M. A., Moritz, M. A., Parisien, M. A., Van Dorn, J., and Hayhoe, K.:
 827 Global Pyrogeography: the Current and Future Distribution of Wildfire, Plos One,
 828 4, e5102, doi: 10.1371/journal.pone.0005102, 2009.
- 829 Langmann, B., Duncan, B., Textor, C., Trentmann, J., and van der Werf, G. R.:
 830 Vegetation fire emissions and their impact on air pollution and climate, Atmos
 831 Environ, 43, 107-116, 2009.
- 832 Lehsten, V., Harmand, P., Palumbo, I., and Arneth, A.: Modelling burned area in
 833 Africa, Biogeosciences, 7, 3199-3214, 2010.
- 834 Marlon, J. R., Bartlein, P. J., Carcaillet, C., Gavin, D. G., Harrison, S. P., Higuera, P.
 835 E., Joos, F., Power, M. J., and Prentice, I. C.: Climate and human influences on
 836 global biomass burning over the past two millennia, Nature Geosci., 1, 697-702,
 837 2008.
- 838 Moritz, M. A., Batllori, E., Bradstock, R. A., Gill, A. M., Handmer, J., Hessburg, P.
 839 F., Leonard, J., McCaffrey, S., Odion, D. C., and Schoennagel, T.: Learning to
 840 coexist with wildfire, Nature, 515, 58-66, 2014.
- 841 Niemi, J. V., Tervahattu, H., Vehkamäki, H., Martikainen, J., Laakso, L., Kulmala,
 842 M., Aarnio, P., Koskentalo, T., Sillanpää, M., and Makkonen, U.: Characterization
 843 of aerosol particle episodes in Finland caused by wildfires in Eastern Europe,
 844 Atmos Chem Phys, 5, 2299-2310, 2005.



- 845 Page, S. E., Siegert, F., Rieley, J., Boehm, H.-D., Jayak, A., and Limink, S.: The
846 amount of carbon released from peat and forest fires in Indonesia during 1997,
847 Nature, 420, 61-65, 2002.
- 848 Prestele, R., Alexander, P., Rounsevell, M. D. A., Arneth, A., Calvin, K., Doelman, J.,
849 Eitelberg, D. A., Engström, K., Fujimori, S., and Hasegawa, T.: Hotspots of
850 uncertainty in land-use and land-cover change projections: a global-scale model
851 comparison, Global Change Biology, 2016. 2016.
- 852 Randerson, J., Chen, Y., van der Werf, G. R., Rogers, B. M., and Morton, D. C.:
853 Global burned area and biomass burning emissions from small fires, J. Geophys.
854 Res., 117, G04012, 2012.
- 855 Shu, L., Tian X., and Wang, M.: A study on forest fire occurrence in China. XII
856 World Forestry Congress, Québec City, Canada, 21–28 September,
857 <http://www.fao.org/docrep/ARTICLE/WFC/XII/0278-B1.HTM>, 2003.
- 858 Smith, B., Prentice, C., and Sykes, M.: Representation of vegetation dynamics in
859 modelling of terrestrial ecosystems: comparing two contrasting approaches within
860 European climate space, Global Ecol Biogeogr, 10, 621-637, 2001.
- 861 Sofiev, M., Ermakova, T., and Vankevich, R.: Evaluation of the smoke-injection
862 height from wild-land fires using remote-sensing data, Atmos Chem Phys, 12,
863 1995-2006, 2012.
- 864 Stohl, A., Aamaas, B., Amann, M., Baker, L., Bellouin, N., Berntsen, T., Boucher, O.,
865 Cherian, R., Collins, W., and Daskalakis, N.: Evaluating the climate and air quality
866 impacts of short-lived pollutants, Atmos Chem Phys, 15, 10529-10566, 2015.
- 867 Tai, A. P. K., Mickley, L. J., and Jacob, D. J.: Correlations between fine particulate
868 matter (PM 2.5) and meteorological variables in the United States: Implications for
869 the sensitivity of PM 2.5 to climate change, Atmos Environ, 44, 3976-3984, 2010.



- 870 Taylor, K. E., Stouffer, R. J., and Meehl, G. A.: An overview of CMIP5 and the
871 experiment design, *Bull. Am. Meteorol. Soc.*, 93, 485-498, 2012.
- 872 van der Werf, G. R., Randerson, J. T., Giglio, L., Collatz, G. J., Mu, M., Kasibhatla,
873 P. S., Morton, D. C., Defries, R. S., Jin, Y., and van Leeuwen, T. T.: Global fire
874 emissions and the contribution of deforestation, savanna, forest, agricultural, and
875 peat fires (1997-2009), *Atmos. Chem. Phys.*, 10, 11707-11735, 2010.
- 876 van der Werf, G. R., Peters, W., van Leeuwen, T. T., and Giglio, L.: What could have
877 caused pre-industrial biomass burning emissions to exceed current rates?, *Clim.*
878 *Past*, 9, 289-306, 2013.
- 879 van Vuuren, A. J., Edmonds, J., Kainuma, M., Riahi, K., Thomson, A., Hibbard, K.,
880 Hurtt, G. C., Kram, T., Krey, V., Lamarque, J. F., Masui, T., Meinshausen, M.,
881 Naicenovic, N., Smith, S. J., and Rose, S. K.: The representative concentration
882 pathways: an overview, *Clim. Change*, 109, 5-31, 2011.
- 883 Veira, A., Kloster, S., Wilkenskjeld, S., and Remy, S.: Fire emission heights in the
884 climate system–Part 1: Global plume height patterns simulated by ECHAM6-
885 HAM2, *Atmos Chem Phys*, 15, 7155-7171, 2015.
- 886 Wang, Z., Chappellaz, J., Park, K., and Mak, J. E.: Large variations in Southern
887 Hemisphere biomass burning during the last 650 years, *Science*, 330, 1663-1666,
888 2010.
- 889 Westerling, A. L. R.: Increasing western US forest wildfire activity: sensitivity to
890 changes in the timing of spring, *Phil. Trans. R. Soc. B*, 371, 20150178, 2016.
- 891 WHO: Air quality guidelines for particulate matter, ozone, nitrogen dioxide and sulfur
892 dioxide, Global update 2005, Summary of risk assessment, World Health
893 Organization 2006.
- 894 Wooster, M. J., Roberts, G., Perry, G. L. W., and Kaufman, Y. L.: Retrieval of



895 biomass combustion rates and totals from fire radiative power observations: FRP
896 derivation and calibration relationships between biomass consumption and fire
897 radiative energy release, J Geophys Res, 110, doi:10.1029/2005JD006318, 2005.



898 **Tables**

899 *Table 1: Emissions [Gg/yr] by world region from various sources*

| Region | PM2.5 | | | NOx | | |
|---------------------------------------|-----------------------|----------------------------|------------------------|-----------------------|----------------------------|------------------------|
| | Wildfire ¹ | Deforestation ¹ | Peat fire ¹ | Wildfire ¹ | Deforestation ¹ | Peat fire ¹ |
| Sub-Saharan Africa | 14,973 | 538 | 0 | 8,141 | 151 | 0 |
| Latin America & Caribbean | 3,138 | 1,886 | 0 | 1,655 | 528 | 0 |
| Easter Europe-Russia-Central Asia | 2,832 | 0 | 18 | 265 | 0 | 9 |
| South & Southeast Asia | 1,593 | 1,499 | 598 | 791 | 420 | 297 |
| Australia & New Zealand | 1,536 | 22 | 0 | 747 | 6 | 0 |
| North America | 1,349 | 0 | 30 | 126 | 0 | 15 |
| Developing East Asia | 364 | 17 | 0 | 73 | 5 | 0 |
| High-income Europe | 31 | 0 | 0 | 13 | 0 | 0 |
| Developing Middle East & North Africa | 7 | 0 | 0 | 4 | 0 | 0 |
| Globe | 25,842 | 3,968 | 646 | 11,822 | 1,112 | 321 |
| CO | | | | | | |
| Sub-Saharan Africa | 131,545 | 5,500 | 0 | 773 | 31 | 0 |
| Latin America & Caribbean | 27,315 | 19,270 | 0 | 160 | 108 | 0 |
| Easter Europe-Russia-Central Asia | 23,461 | 0 | 286 | 97 | 0 | 2 |
| South & Southeast Asia | 13,623 | 15,319 | 9,739 | 80 | 86 | 72 |
| Australia & New Zealand | 13,056 | 221 | 0 | 76 | 1 | 0 |
| North America | 10,976 | 0 | 496 | 46 | 0 | 4 |
| Developing East Asia | 2,886 | 173 | 3 | 14 | 1 | 0 |
| High-income Europe | 250 | 0 | 0 | 1 | 0 | 0 |
| Developing Middle East & North Africa | 59 | 0 | 0 | 0 | 0 | 0 |
| Globe | 223,331 | 40,557 | 10,524 | 1,249 | 227 | 77 |
| BC | | | | | | |
| Sub-Saharan Africa | 131,545 | 5,500 | 0 | 773 | 31 | 0 |
| Latin America & Caribbean | 27,315 | 19,270 | 0 | 160 | 108 | 0 |
| Easter Europe-Russia-Central Asia | 23,461 | 0 | 286 | 97 | 0 | 2 |
| South & Southeast Asia | 13,623 | 15,319 | 9,739 | 80 | 86 | 72 |
| Australia & New Zealand | 13,056 | 221 | 0 | 76 | 1 | 0 |
| North America | 10,976 | 0 | 496 | 46 | 0 | 4 |
| Developing East Asia | 2,886 | 173 | 3 | 14 | 1 | 0 |
| High-income Europe | 250 | 0 | 0 | 1 | 0 | 0 |
| Developing Middle East & North Africa | 59 | 0 | 0 | 0 | 0 | 0 |
| Globe | 223,331 | 40,557 | 10,524 | 1,249 | 227 | 77 |

900 ¹GFED4.1s

901 ²ECLIPSE-GAINS 4a



Table 2: Global population affected by wildfire PM_{2.5} emissions above given limit.

| Population | Urbanization | RCP4.5 | | | | | RCP8.5 | | | | |
|---|--------------|---------|-----------------|------|-----|------|--------|------|------|------|-----|
| Limit [g m ⁻² yr ⁻¹] | | Current | % ¹⁾ | 2030 | % | 2050 | % | 2090 | % | 2030 | % |
| 0.2 | | | | | | | | | | | |
| SSP5 | fast | | | 721 | 8.6 | 892 | 10.0 | 1054 | 12.5 | 721 | 8.6 |
| SSP2 | fast | | | 771 | 8.9 | 1032 | 10.6 | 1498 | 14.5 | 775 | 8.9 |
| SSP2 | central | 568 | 7.9 | 780 | 9.0 | 1042 | 10.7 | 1466 | 14.2 | 782 | 9.0 |
| SSP2 | slow | | | 787 | 9.1 | 1045 | 10.8 | 1468 | 14.3 | 785 | 9.0 |
| SSP3 | slow | | | 844 | 9.3 | 1302 | 12.1 | 2221 | 16.0 | 842 | 9.3 |
| 0.5 | | | | | | | | | | | |
| Limit [g m ⁻² yr ⁻¹] | | | | | | | | | | | |
| SSP5 | fast | | | 313 | 3.7 | 384 | 4.3 | 456 | 5.4 | 317 | 3.8 |
| SSP2 | fast | | | 333 | 3.8 | 441 | 4.5 | 646 | 6.3 | 337 | 3.9 |
| SSP2 | central | 256 | 3.6 | 340 | 3.9 | 446 | 4.6 | 636 | 6.2 | 341 | 3.9 |
| SSP2 | slow | | | 349 | 4.0 | 455 | 4.7 | 629 | 6.1 | 348 | 4.0 |
| SSP3 | slow | | | 372 | 4.1 | 531 | 4.9 | 911 | 6.6 | 374 | 4.1 |
| 1 | | | | | | | | | | | |
| Limit [g m ⁻² yr ⁻¹] | | | | | | | | | | | |
| SSP5 | fast | | | 146 | 1.7 | 176 | 2.0 | 204 | 2.4 | 148 | 1.8 |
| SSP2 | fast | | | 154 | 1.8 | 193 | 2.0 | 280 | 2.7 | 155 | 1.8 |
| SSP2 | central | 126 | 1.8 | 156 | 1.8 | 187 | 1.9 | 267 | 2.6 | 158 | 1.8 |
| SSP2 | slow | | | 162 | 1.9 | 194 | 2.0 | 247 | 2.4 | 162 | 1.9 |
| SSP3 | slow | | | 173 | 1.9 | 211 | 2.0 | 330 | 2.4 | 172 | 1.9 |

¹⁾ Per cent of global population

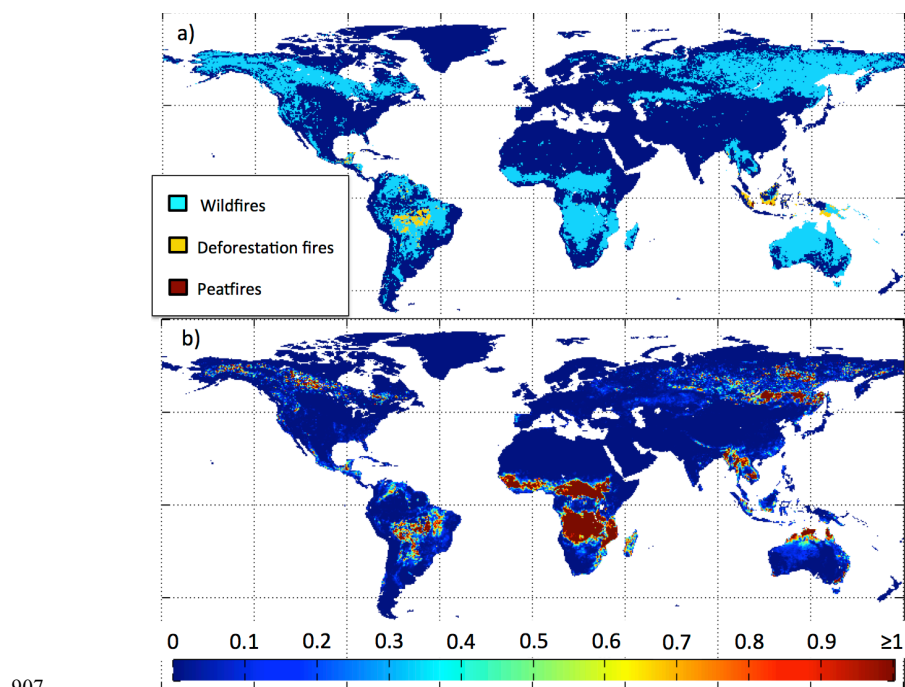


905 Table 3: Average annual exposure of population to $PM_{2.5}$ [$\mu g\ m^{-3}$] under idealized conditions.

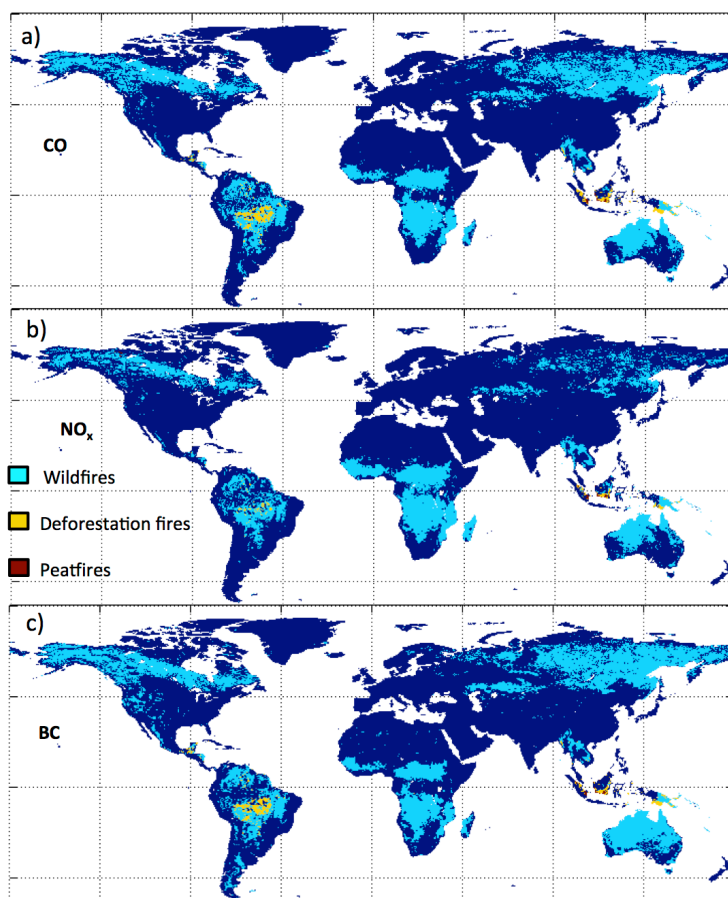
| Population | Urbanization | Current | RCP4.5 | | RCP8.5 | |
|-----------------------------|--------------|---------|--------|------|--------|------|
| | | | 2030 | 2050 | 2030 | 2050 |
| Sub-Saharan Africa | | | | | | |
| SSP5 | fast | | 6.6 | 6.5 | 6.4 | 6.3 |
| SSP2 | fast | | 6.5 | 6.2 | 6.0 | 6.0 |
| SSP2 | central | 7.7 | 6.5 | 6.0 | 5.7 | 5.9 |
| SSP2 | slow | | 6.4 | 5.8 | 5.4 | 5.7 |
| SSP3 | slow | | 6.3 | 5.6 | 5.1 | 5.5 |
| Australia and New Zealand | | | | | | |
| SSP5 | fast | | 3.2 | 3.5 | 3.6 | 3.5 |
| SSP2 | fast | | 3.2 | 3.5 | 3.6 | 3.5 |
| SSP2 | central | 3.1 | 3.2 | 3.5 | 3.6 | 3.5 |
| SSP2 | slow | | 3.2 | 3.5 | 3.6 | 3.5 |
| SSP3 | slow | | 3.2 | 3.5 | 3.7 | 3.5 |
| Latin America and Caribbean | | | | | | |
| SSP5 | fast | | 1.5 | 1.6 | 1.7 | 1.6 |
| SSP2 | fast | | 1.5 | 1.5 | 1.6 | 1.6 |
| SSP2 | central | 1.5 | 1.5 | 1.5 | 1.6 | 1.6 |
| SSP2 | slow | | 1.5 | 1.5 | 1.6 | 1.6 |
| SSP3 | slow | | 1.5 | 1.5 | 1.5 | 1.5 |



906 Figures



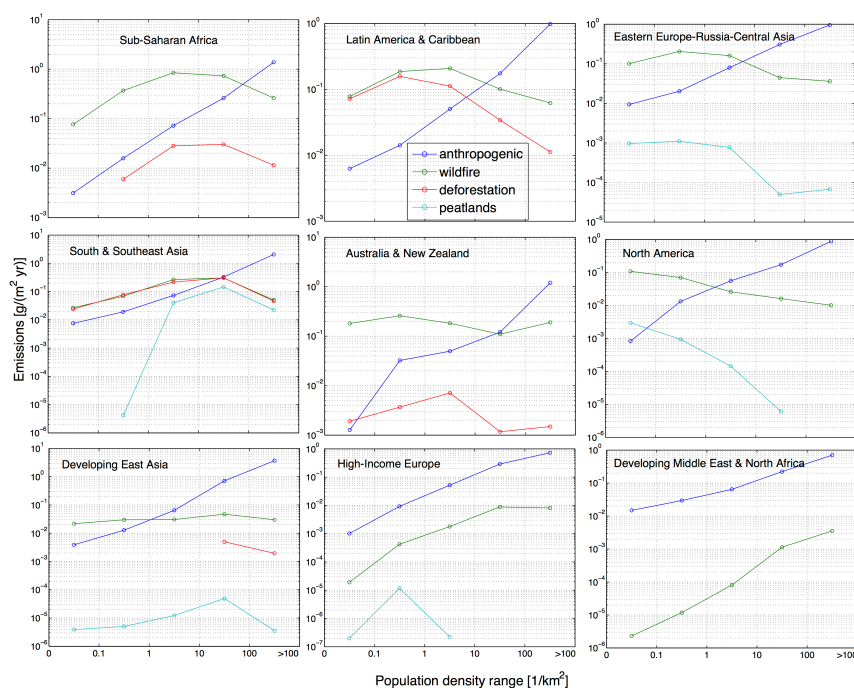
908 *Figure 1: a) Largest current source of PM_{2.5} emissions, including anthropogenic*
 909 *sources (dark blue areas); b) wildfires emissions in g PM_{2.5} m⁻² yr⁻¹. Average annual*
 910 *PM_{2.5} emissions 1997 to 2014 are from GFED4.1s, or ECLIPSE GAINS 4a for*
 911 *2010 (anthropogenic).*



912

913 *Figure 2: Largest current source of annual air pollutant emissions. Dark blue areas:*

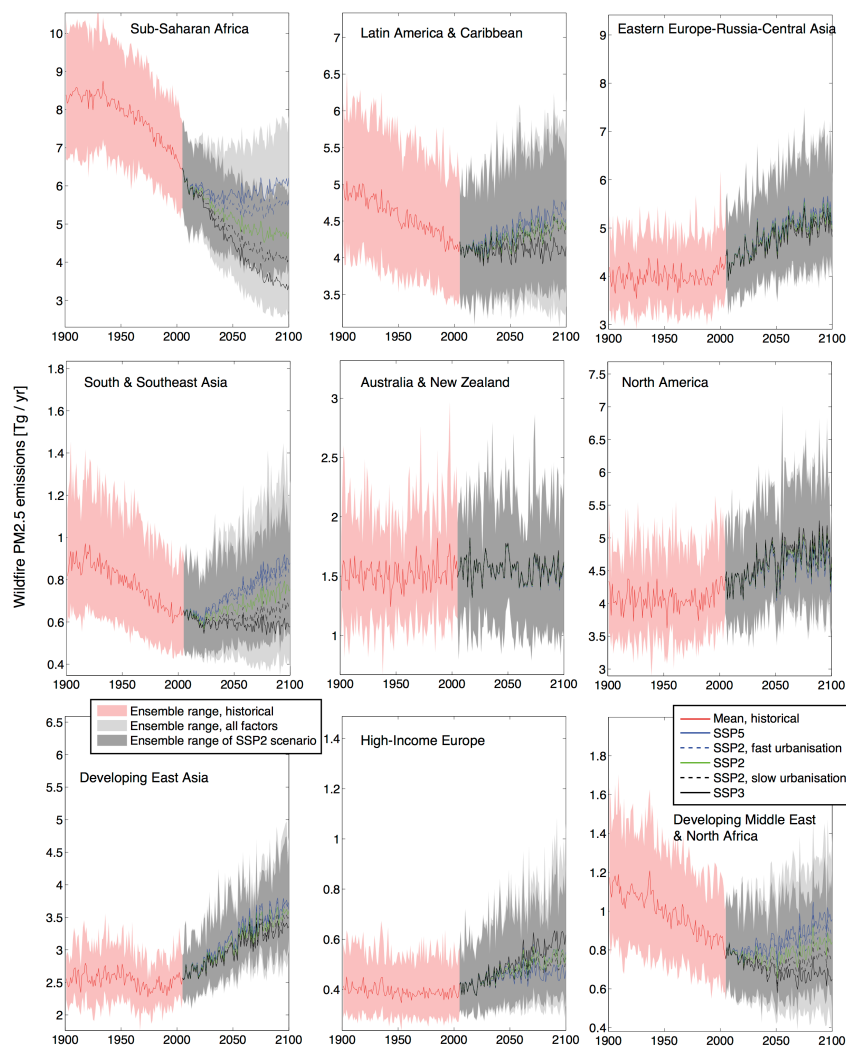
914 *dominant source anthropogenic, or zero emissions. a) CO, b) NO_x, c) black carbon.*



915

916 *Figure 3: Comparison of current anthropogenic, wildfire, deforestation fire and peat*
 917 *fire PM_{2.5} emissions by region and range population density, constructed by relating*
 918 *emission rates to the population density found for the same grid box on a 0.5 by 0.5*
 919 *degree grid. Emissions are from ECLIPSE GAINS 4a (anthropogenic source for*
 920 *2010) and GFED4.1s (average of 1997-2014).*

921



922

923 *Figure 4. Annual PM_{2.5} emissions from ensemble of LPJ-GUESS-SIMFIRE*

924 *simulations for nine world regions 1901 to 2100. Ensemble ranges and impact of*

925 *population and urbanisation scenarios. Climate scenario: RCP4.5.*

926

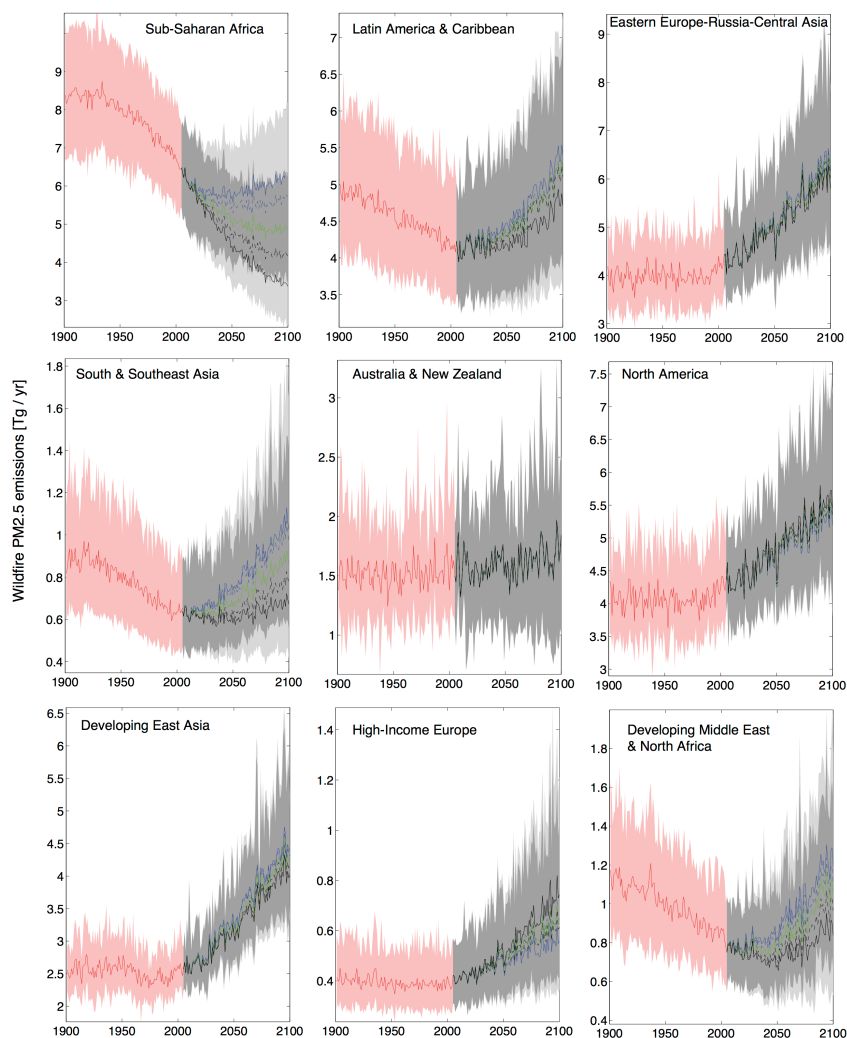
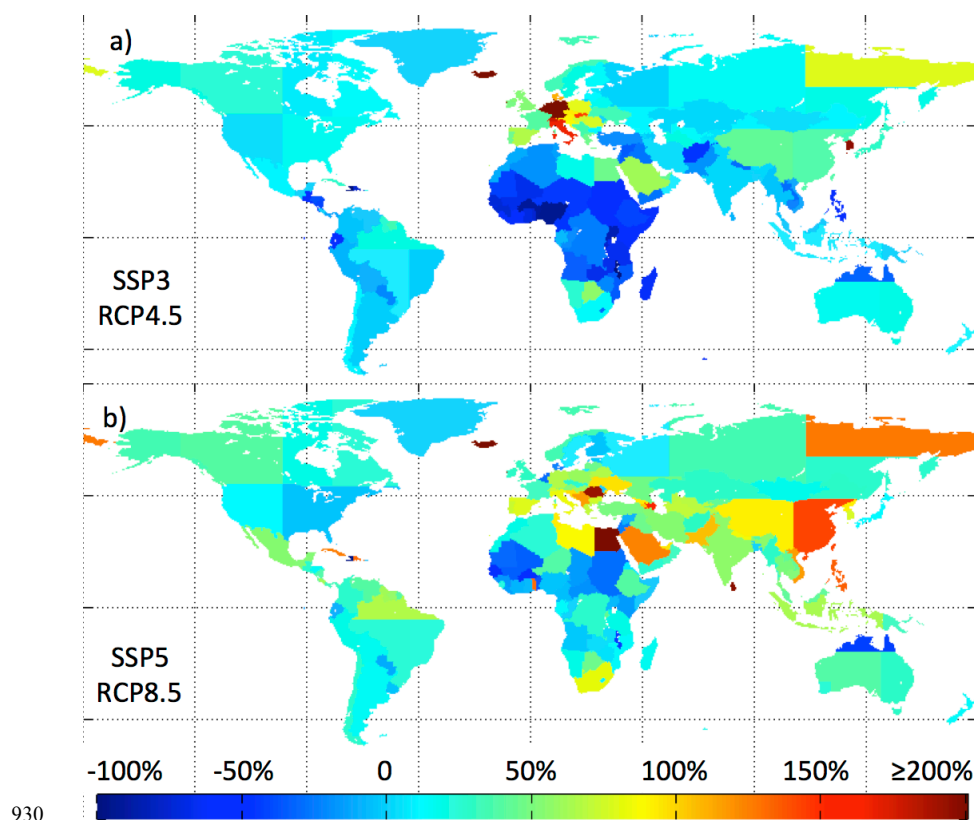
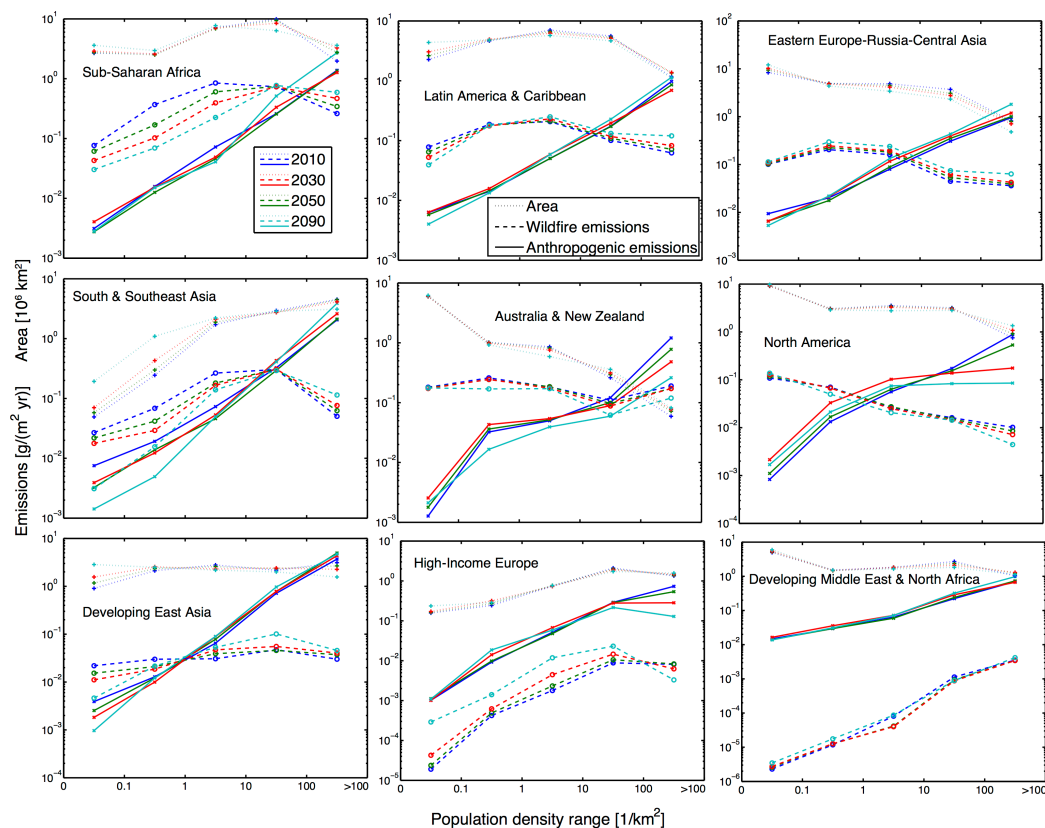


Figure 5. Same as previous figure, but for climate scenario RCP8.5.



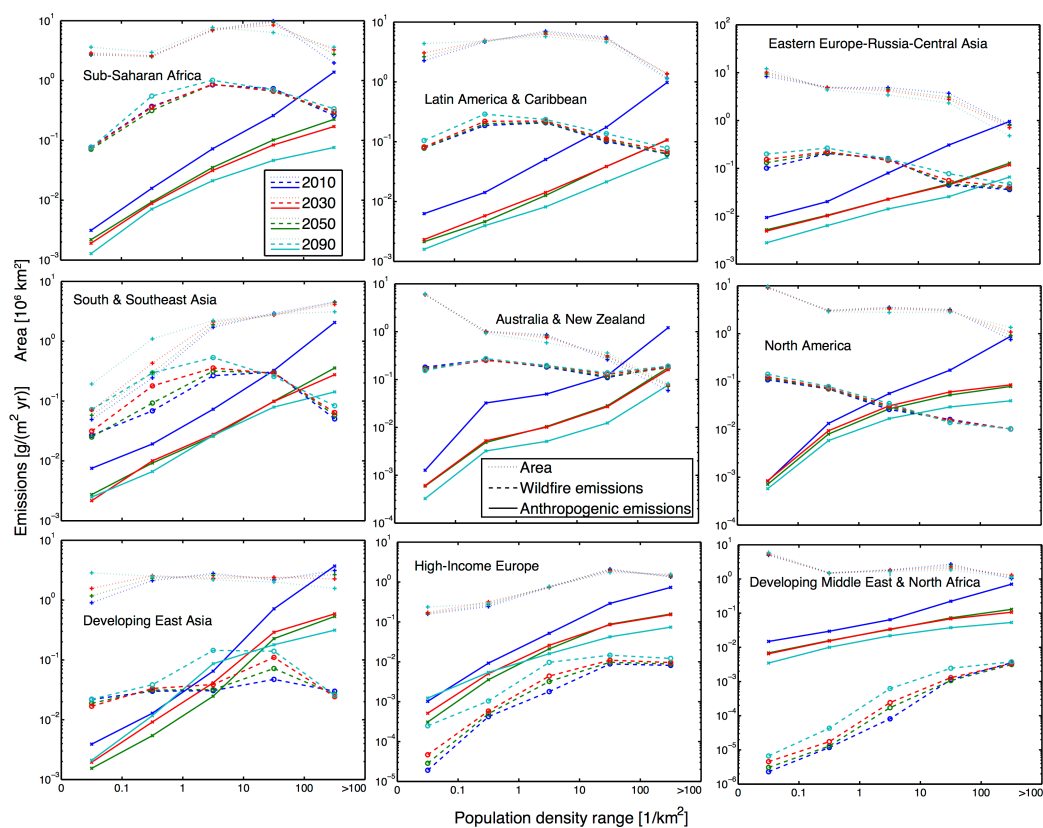
931 *Figure 6: Relative change in annual PM_{2.5} emissions from current (1997-2014 mean)*
 932 *to 2090 (2080 to 2100 mean) by country/region. a) SSP3 globally high population*
 933 *growth (high-income countries: low population growth) with slow urbanisation and*
 934 *RCP4.5 climate scenario, b) SSP5 globally low population growth (high-income*
 935 *countries: high population growth) with slow urbanisation, RCP8.5 climate scenario.*



936

937 *Figure 7: Predicted changes of annual PM_{2.5} emissions against ranges of population density from*
 938 *wildfires and anthropogenic sources, as well as changes in area extent of the population-density*
 939 *categories, for the nine world regions, based on re-scaled GFED4.1s wildfire emissions. SSP3*
 940 *demographic scenario, RCP4.5 climate change and Current-Legislation (CLE) anthropogenic*
 941 *emissions scenario.*

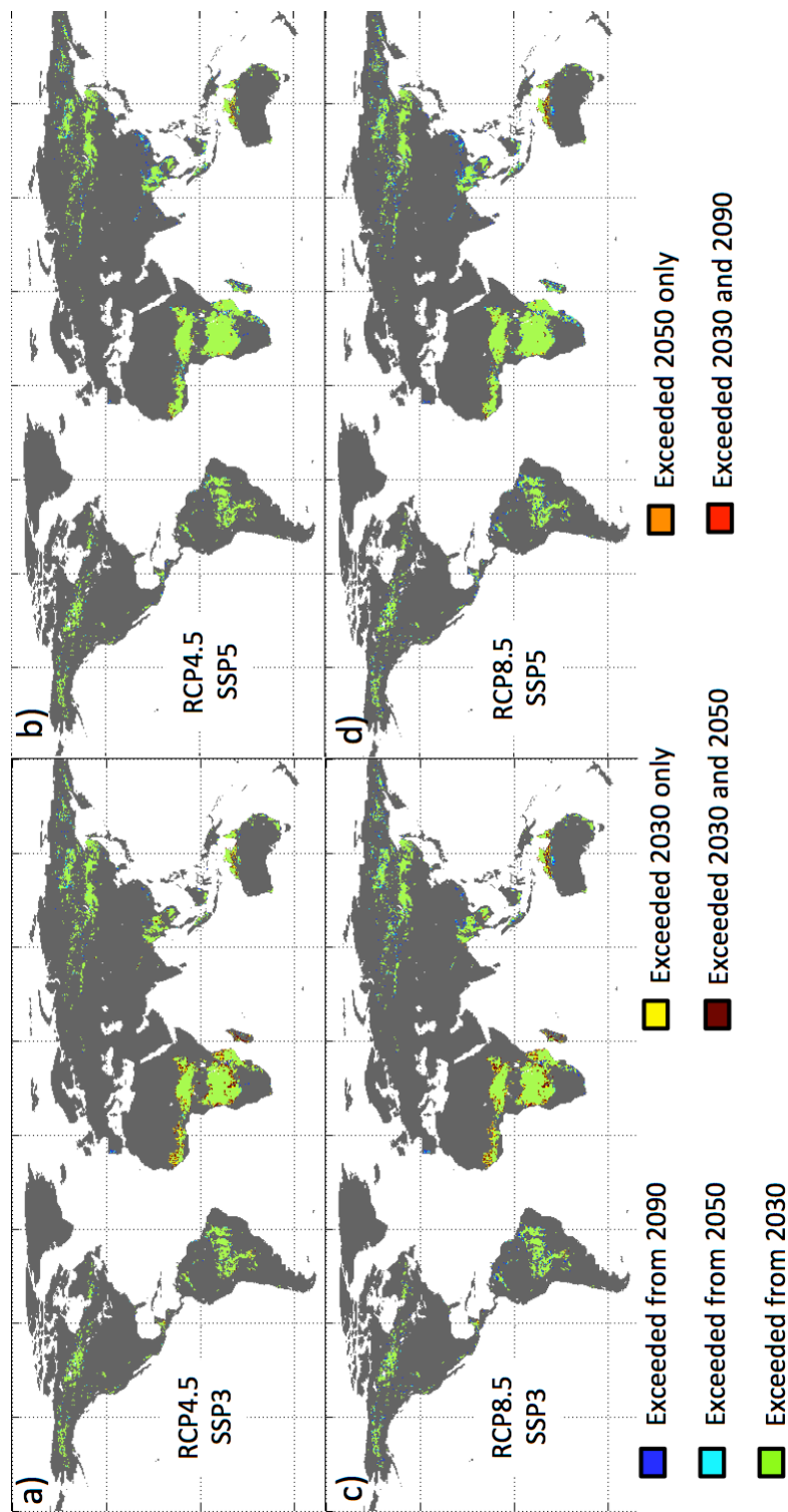
942



943

944 *Figure 8: As previous figure, but for SSP5 demographic scenario, RCP8.5 climate change and*

945 *Maximum Feasible Reduction (MFR) anthropogenic-emissions scenario.*



946

947 *Figure 9: Timing of when annual wildfire emissions exceed $0.5 \text{ g PM}_{2.5} \text{ m}^{-2} \text{ yr}^{-1}$ for the time windows 2030, 2050 and 2090a, b) RCP4.5 and c,*
948 *d) RCP8.5 climate scenario; a, c) SSP3 and b, d) SSP5 demographic scenario.*



949 Appendix

950 *Table A1: Countries/regions used for scaling GFED4.1s wildfire emissions.*

| Code | Country name | World region | grid cells on 1-degree grid | non-crop cells ¹ | Code | Country name | World region | grid cells on 1-degree grid | non-crop cells | longitude range | latitude range |
|------|--------------------------|---|-----------------------------|-----------------------------|--------|---------------------------------------|------------------------------|-----------------------------|----------------|------------------|----------------|
| AGO | Angola | | 100 | 100 | ARM | Armenia | | 4 | 4 | | |
| BEN | Benin | | 10 | 6 | AZE | Azerbaijan | | 7 | 6 | | |
| BWA | Botswana | | 46 | 46 | GEO | Georgia | | 6 | 6 | | |
| BFA | Burkina Faso | | 23 | 21 | KAZ | Kazakhstan | | 213 | 206 | | |
| BDI | Burundi | | 3 | 3 | KGZ | Kyrgyzstan | | 16 | 16 | | |
| CMR | Cameroon | | 37 | 35 | TJK | Tajikistan | | 8 | 8 | | |
| CAF | Central African Republic | | 49 | 46 | TKM | Turkmenistan | | 35 | 35 | | |
| TCO | Chad | | 100 | 100 | UZB | Uzbekistan | | 35 | 32 | | |
| COG | Congo | | 24 | 24 | BLR | Belarus | Eastern Europe, | 16 | 14 | | |
| ZAR | Congo, Dem. Republic | | 176 | 176 | BGR | Bulgaria | Europe, | 10 | 8 | | |
| CIV | Cote d'Ivoire | | 25 | 24 | LLI | Latvia and Lithuania | Russia and Central Asia | 10 | 5 | | |
| ERI | Eritrea | | 12 | 12 | ROM | Romania | | 19 | 10 | | |
| ETH | Ethiopia | | 90 | 89 | RUS-SW | | | 78 | 32 | W of 60°E | S of 52°N |
| GAB | Gabon | | 20 | 20 | RUS-NW | | | 212 | 150 | W of 55°E | N of 52°N |
| GHA | Ghana | | 18 | 13 | RUS-C | Russian Federation | | 553 | 506 | not in other RUS | |
| GIN | Guinea | | 20 | 20 | RUS-SE | | | 232 | 232 | E of 110°E | S of 60°N |
| GNB | Guinea-Bissau | | 1 | 1 | RUS-NE | | | 327 | 327 | E of 110°E | N of 60°N |
| KEN | Kenya | Sub-Saharan Africa | 41 | 40 | UKR | Ukraine | | 47 | 5 | | |
| LSO | Lesotho | | 1 | 1 | YUA | Serbia, Montenegro, Bosnia, Macedonia | | 13 | 11 | | |
| LBR | Liberia | | 5 | 5 | CHN-W | | | 348 | 342 | W of 105°E | |
| MDG | Madagascar | | 43 | 43 | CHN-E | China | Developing East Asia | 283 | 211 | E of 105°E | S of 43°N |
| MWI | Malawi | | 10 | 10 | CHN-N | | | 122 | 103 | | N of 43°N |
| MLI | Mali | | 106 | 106 | PRK | North Korea | | 10 | 8 | | |
| MRT | Mauritania | | 80 | 80 | MNG | Mongolia | | 131 | 131 | | |
| MOZ | Mozambique | | 61 | 60 | BTN | Bhutan | | 4 | 2 | | |
| NAM | Namibia | | 66 | 66 | KHM | Cambodia | | 14 | 13 | | |
| NER | Niger | | 94 | 80 | IND | India | | 256 | 50 | | |
| NGA | Nigeria | | 74 | 40 | IDN | Indonesia | | 125 | 116 | | |
| SEN | Senegal | | 17 | 16 | LAO | Laos | | 18 | 18 | | |
| SLE | Sierra Leone | | 5 | 5 | MYS | Malaysia | South and South-East Asia | 23 | 23 | | |
| SOM | Somalia | | 55 | 55 | MMR | Myanmar | | 44 | 36 | | |
| ZAF | South Africa | | 99 | 98 | NPL | Nepal | | 12 | 8 | | |
| SDN | Sudan | | 207 | 199 | PAK | Pakistan | | 58 | 44 | | |
| TGO | Togo | | 2 | 1 | PHL | Philippines | | 16 | 14 | | |
| UGA | Uganda | | 16 | 13 | LKA | Sri Lanka | | 4 | 4 | | |
| TZA | Tanzania | | 73 | 72 | THA | Thailand | | 42 | 30 | | |
| ZMB | Zambia | | 63 | 63 | VNM | Viet Nam | | 27 | 22 | | |
| ZWE | Zimbabwe | | 30 | 30 | PNG | Papua New Guinea | | 31 | 31 | | |
| DZA | Algeria | | 189 | 184 | AUS-SW | | | 18 | 16 | W of 120°E | S of 30°S |
| EGY | Egypt | | 77 | 76 | AUS-E | Australia | Australia and New Zealand | 200 | 178 | E of 140°E | S of 18°S |
| LBY | Libya | | 131 | 131 | AUS-C | | | 317 | 316 | not in other AUS | |
| MAR | Morocco | | 56 | 49 | AUS-N | | | 76 | 76 | | N of 18°S |
| TUN | Tunisia | | 14 | 11 | NZL | New Zealand | | 22 | 22 | | |
| AFG | Afghanistan | Developing Middle East and North Africa | 53 | 52 | CAN-W | | | 385 | 341 | W of 100°W | |
| IRN | Iran | | 134 | 129 | CAN-C | Canada | | 192 | 185 | 100...80°W | |
| IRQ | Iraq | | 37 | 31 | CAN-E | | | 176 | 176 | E of 80°W | |
| JOR | Jordan | | 6 | 6 | USA-W | United States of America | North America | 314 | 294 | W of 100°W | |
| SAU | Saudi Arabia | | 154 | 154 | USA-E | | | 372 | 222 | E of 100°W | |
| SYR | Syria | | 15 | 9 | ALK | | | 116 | 116 | | N of 50°N |
| TUR | Turkey | | 57 | 44 | CRI | Costa Rica | | 3 | 3 | | |
| YEM | Yemen | | 31 | 31 | CUB | Cuba | | 7 | 5 | | |
| AUT | Austria | | 7 | 7 | DOM | Dominican Republic | | 4 | 4 | | |
| BNL | Benelux | | 5 | 3 | GTM | Guatemala | | 15 | 15 | | |
| CRS | Croatia and Slovenia | | 3 | 2 | HTI | Haiti | | 2 | 2 | | |
| CZE | Czech Republic | | 5 | 3 | HND | Honduras | | 9 | 9 | | |
| DNK | Denmark | | 6 | 3 | MEX-W | Mexico | | 120 | 115 | W of 95°W | |
| EST | Estonia | | 4 | 4 | MEX-SE | | | 19 | 19 | E of 95°W | |
| FIN | Finland | | 28 | 27 | NIC | Nicaragua | | 8 | 8 | | |
| FRA | France | | 41 | 24 | PAN | Panama | | 6 | 6 | | |
| DEU | Germany | | 32 | 29 | ARG | Argentina | | 230 | 207 | | |
| GRC | Greece | | 10 | 9 | BOL | Bolivia | Latina America and Caribbean | 88 | 88 | | |
| HUN | Hungary | High-income Europe | 7 | 2 | BRA-W | Brazil | | 197 | 192 | W of 49°W | S of 5°S |
| ISL | Iceland | | 7 | 7 | BRA-E | | | 316 | 294 | E of 49°W | |
| IRL | Ireland | | 5 | 4 | BRA-N | | | 161 | 161 | | N of 5°S |
| ITA | Italy | | 23 | 11 | CHL | Chile | | 61 | 60 | | |
| NOR | Norway | | 31 | 31 | COL | Colombia | | 88 | 88 | | |
| POL | Poland | | 25 | 11 | ECU | Ecuador | | 19 | 19 | | |
| PRT | Portugal | | 6 | 5 | GUF | French Guiana | | 6 | 6 | | |
| SVK | Slovakia | | 6 | 2 | GUY | Guyana | | 15 | 15 | | |
| ESP | Spain | | 40 | 24 | PRY | Paraguay | | 28 | 28 | | |
| SWE | Sweden | | 39 | 39 | PER | Peru | | 100 | 100 | | |
| CHE | Switzerland | | 2 | 2 | SUR | Suriname | | 11 | 11 | | |
| GBR | United Kingdom | | 19 | 13 | URY | Uruguay | | 15 | 15 | | |
| | | | | | VEN | Venezuela | | 73 | 73 | | |
| | | | | | ISR | Israel | | 4 | 4 | | |
| | | | | | JPN | Japan | | 28 | 28 | | |
| | | | | | KOR | South Korea | | 6 | 6 | | |
| | | | | | OMN | Oman | | 26 | 26 | | |
| | | | | | ARE | United Arab Emirates | | 8 | 8 | | |
| | | | | | MDA | Republic of Moldova ² | | 4 | 0 | | |
| | | | | | BGD | Bangladesh ³ | | 10 | 1 | | |
| | | | | | GRL | Greenland ³ | | 31 | 31 | | |

¹ Cells with less than 50% cropland fraction in past or future scenarios

² Constant emissions assumed because dominated by croplands

³ Constant emissions assumed because zero current wildfire emissions in some simulations

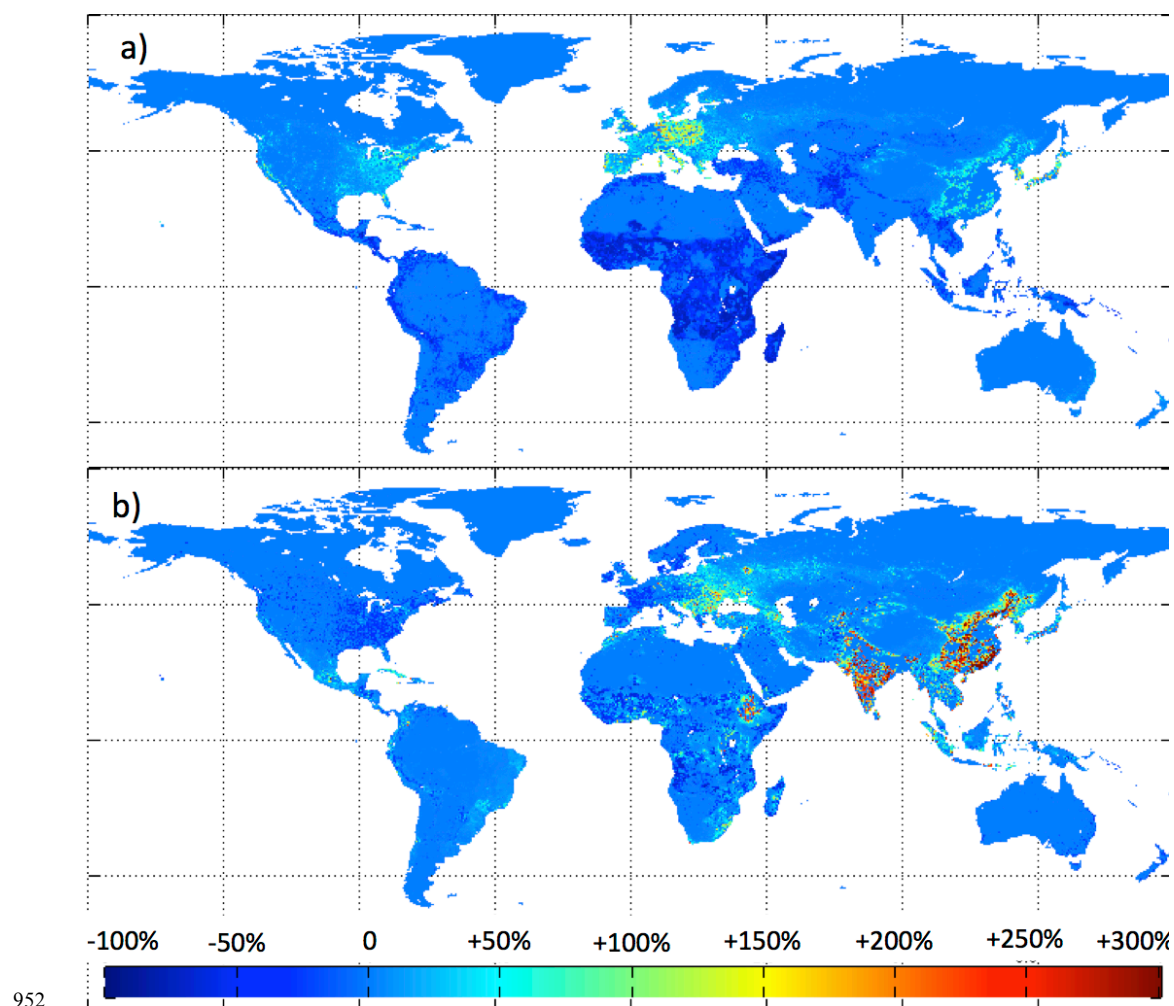
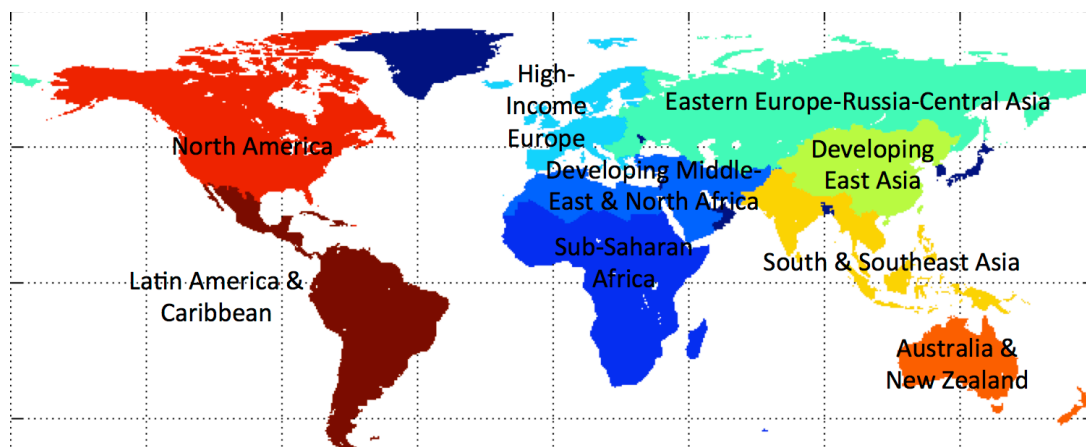
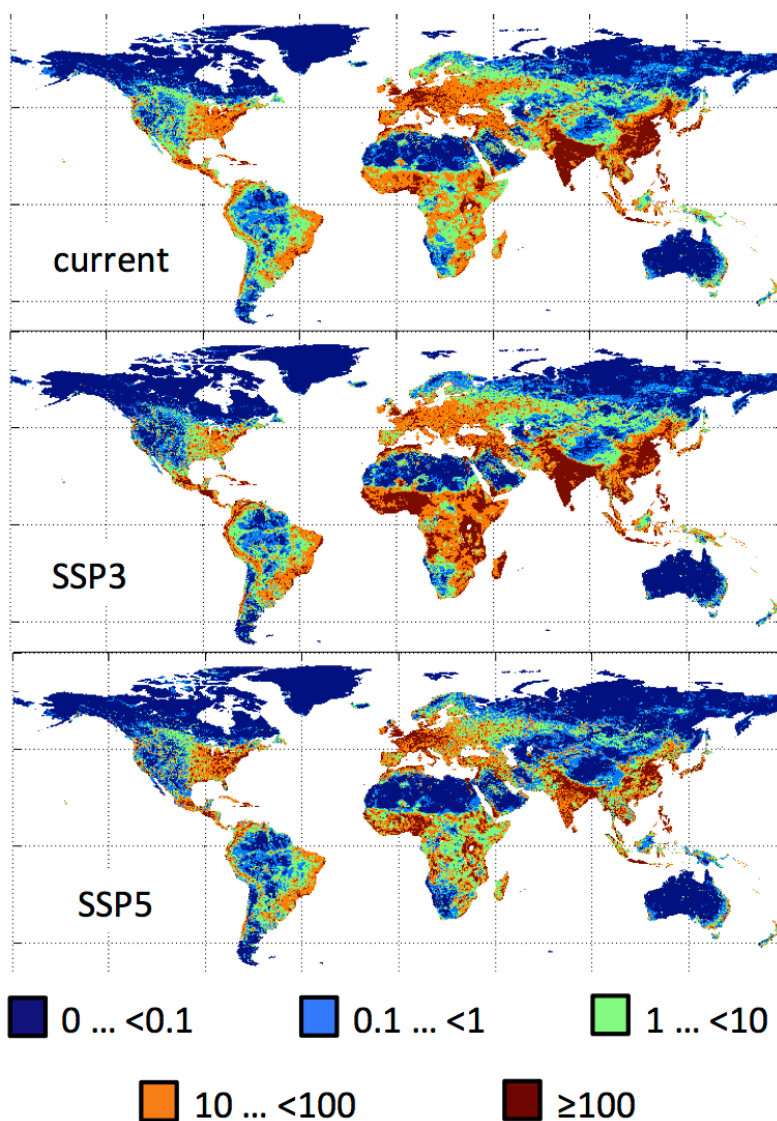


Figure A1: Relative change in wildfire emissions due to changes in population density from 2010 to 2090 according to Equ. 2. a) SSP3, b) SSP5 demographic scenario.



956
 957 *Figure A2: World regions used in the analysis. Dark blue: not included*



958

959 *Figure A3: Population density categories for current (2010) and future (2090) conditions for the SSP3*
 960 *and SSP3 demographic scenarios.*

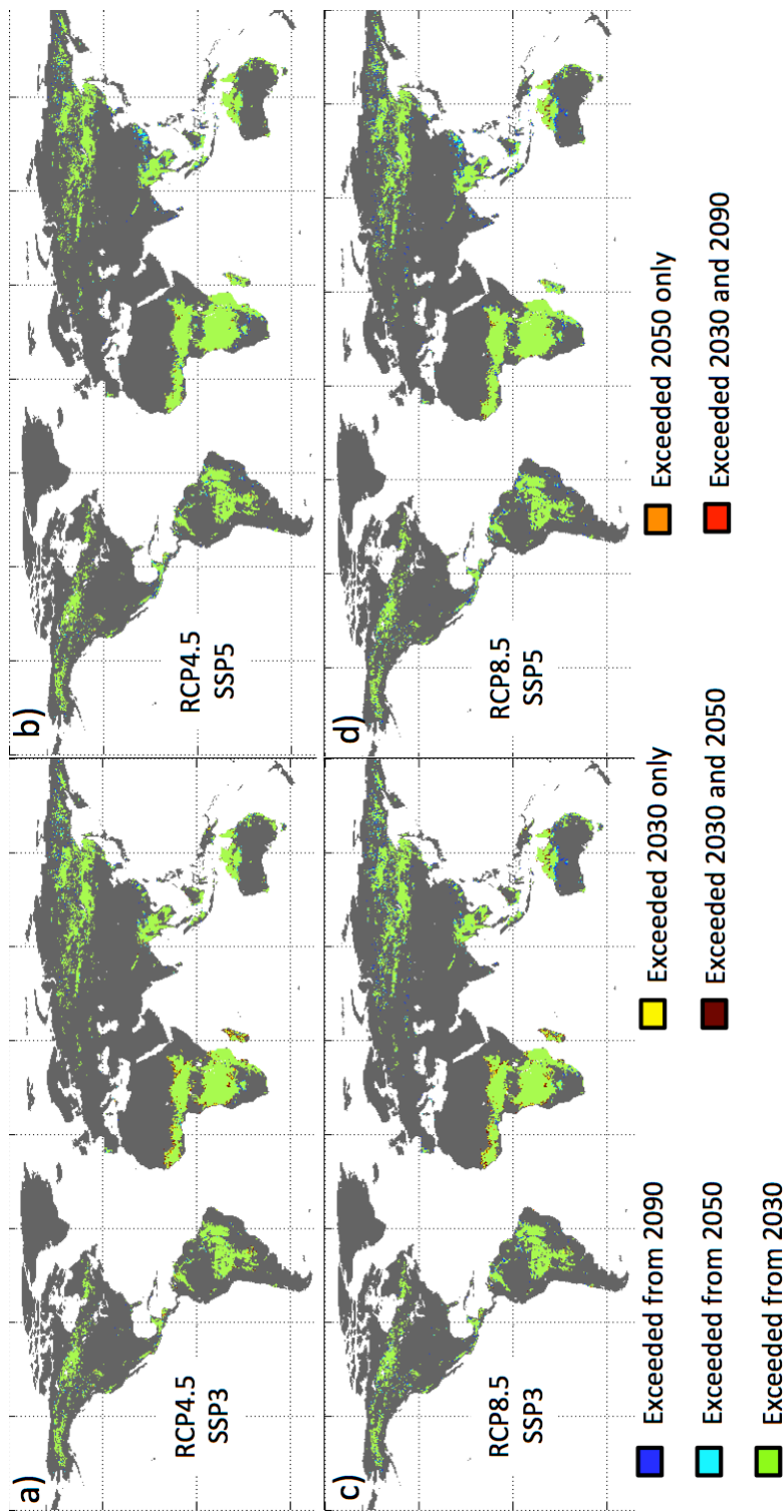


Figure A4: Timing of when annual wildfire emissions exceed $0.2 \text{ g PM}_{2.5} \text{ m}^{-2} \text{ yr}^{-1}$ for the time windows 2030, 2050 and 2090a, b) RCP4.5 and c, d) RCP8.5 climate scenario; a, c) SSP3 and b, d) SSP5 demographic scenario.

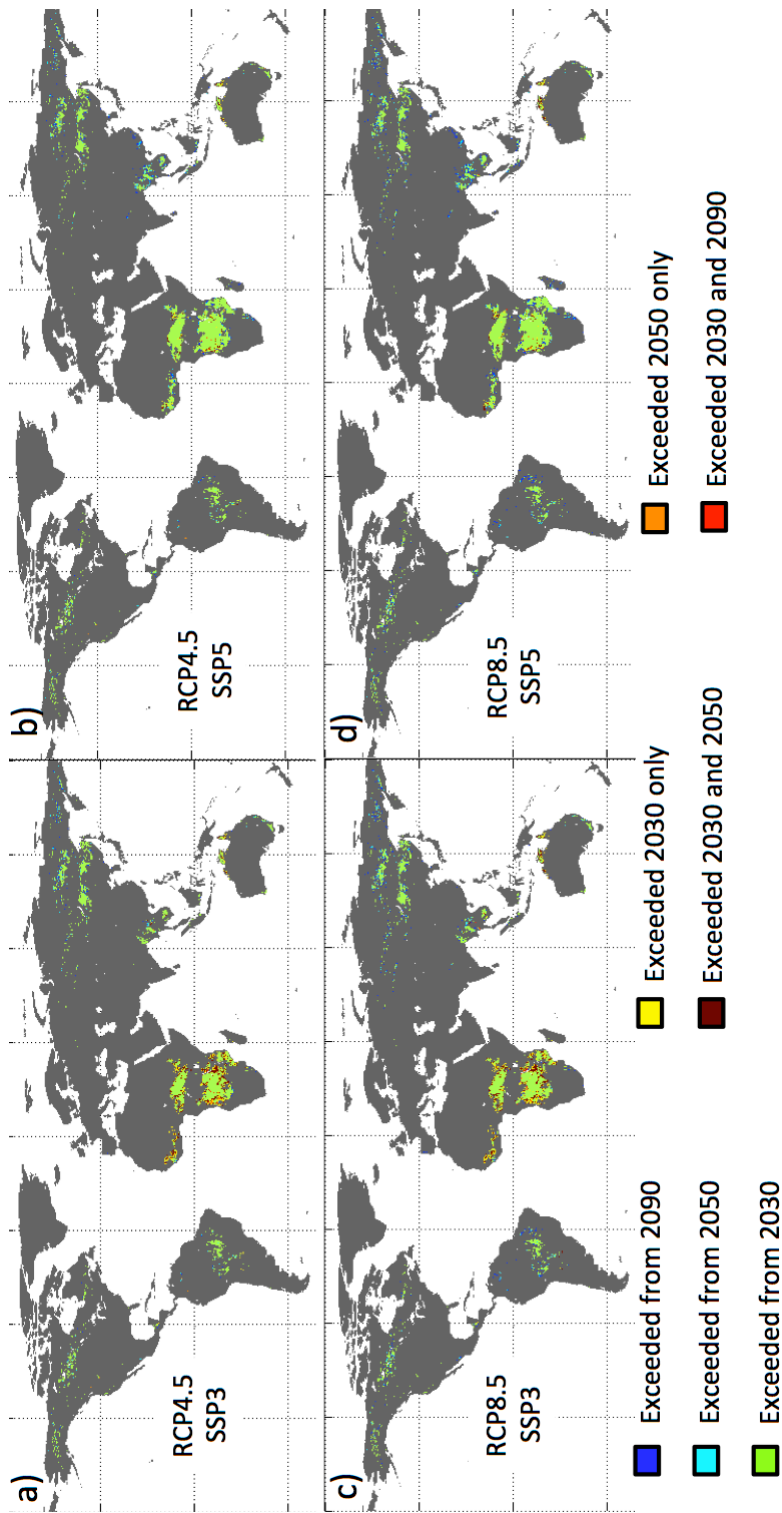
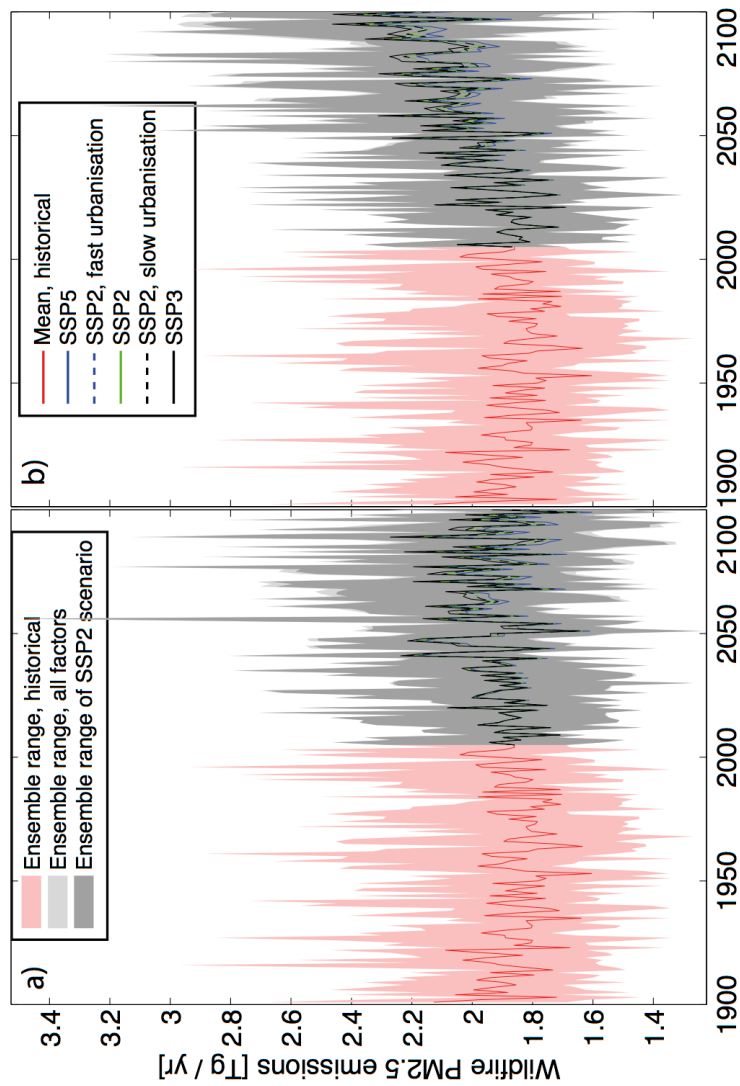


Figure A5: as previous figure, but for a threshold of $1 \text{ g PM}_{2.5} \text{ m}^{-2} \text{ yr}^{-1}$.



967

968 *Figure A6: Simulated annual wildfire PM_{2.5} emissions by LPJ-GUESS-SIMFIRE for the Western U.S. (region USA-W, Table A1).*